



## 저작자표시-비영리-변경금지 2.0 대한민국

이용자는 아래의 조건을 따르는 경우에 한하여 자유롭게

- 이 저작물을 복제, 배포, 전송, 전시, 공연 및 방송할 수 있습니다.

다음과 같은 조건을 따라야 합니다:



저작자표시. 귀하는 원저작자를 표시하여야 합니다.



비영리. 귀하는 이 저작물을 영리 목적으로 이용할 수 없습니다.



변경금지. 귀하는 이 저작물을 개작, 변형 또는 가공할 수 없습니다.

- 귀하는, 이 저작물의 재이용이나 배포의 경우, 이 저작물에 적용된 이용허락조건을 명확하게 나타내어야 합니다.
- 저작권자로부터 별도의 허가를 받으면 이러한 조건들은 적용되지 않습니다.

저작권법에 따른 이용자의 권리는 위의 내용에 의하여 영향을 받지 않습니다.

이것은 [이용허락규약\(Legal Code\)](#)을 이해하기 쉽게 요약한 것입니다.

[Disclaimer](#)

Master's Thesis

ELECTROCHEMICAL ACTIVATION OF  
NITRATE FOR BENZOIC ACID REMOVAL:  
ROLE OF HYDROXYLAMINE

Ki-Myeong Lee

Department of Urban and Environmental Engineering  
(Environmental Science and Engineering)

Graduate School of UNIST

2019

# ELECTROCHEMICAL ACTIVATION OF NITRATE FOR BENZOIC ACID REMOVAL: ROLE OF HYDROXYLAMINE

Ki-Myeong Lee

Department of Urban and Environmental Engineering  
(Environmental Science and Engineering)

Graduate School of UNIST

# ELECTROCHEMICAL ACTIVATION OF NITRATE FOR BENZOIC ACID REMOVAL: ROLE OF HYDROXYLAMINE

A thesis  
submitted to the Graduate School of UNIST  
in partial fulfillment of the  
requirements for the degree of  
Master of Science

Ki-Myeong Lee

01.07.2019 of submission

Approved by



---

Advisor

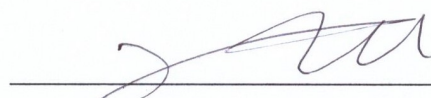
Kyung Hwa Cho

# ELECTROCHEMICAL ACTIVATION OF NITRATE FOR BENZOIC ACID REMOVAL: ROLE OF HYDROXYLAMINE

Ki-Myeong Lee

This certifies that the thesis of Ki-Myeong Lee is approved.

01.07.2019



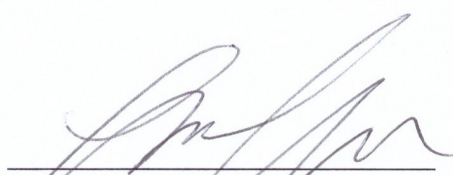
---

Advisor: Kyung Hwa Cho



---

Changsoo Lee



---

Changha Lee

## Abstract

Hydroxylamine (HA) is one of the intermediates produced during the electrochemical nitrate reduction process capable of degrading organic pollutants. Thus, the potential of the electrochemical utilization of HA toward applying it to organic pollutant removal was evaluated. The potential for the electrochemical activation of nitrates for benzoic acid (BA) removal and the role of HA during this process was assessed in this study.

The production of HA during electrochemical nitrate reduction was examined with several cathode materials, namely copper, silver, stainless steel, titanium (Ti), aluminum, nickel, zinc (Zn), and tin (Sn). To compare the performance of the electrodes during HA generation, the selectivity of the reduction products, the nitrate conversion rate, and the Faradaic efficiency of HA were investigated. Although Zn achieved the best nitrate conversion rate (2,566.45 mmol/m<sup>2</sup>/h) and Sn attained the best HA selectivity (64.16%), Ti was found to be the optimal electrode in the electrochemical nitrate activation for the organic pollutant removal process since it obtained the best Faradaic efficiency for HA generation (31%) and the largest HA production (5.82 mM).

The performance of the process was evaluated using BA degradation. Experiments were conducted with three electrolytes: nitrate, perchlorate, and perchlorate with HA. In these experiments, perchlorate electrolyte was used as the control because it is an electrochemically inert electrolyte. In addition, the processes were evaluated according to voltage (1.4–2.2 V vs. a saturated calomel electrode (SCE)). With the nitrate electrolyte, BA degradation drastically enhanced at 1.8 V vs. SCE (1.6 V vs. SCE: 56%, 1.8 V vs. SCE: 86%) and HA also started to accumulate in the reactor. Furthermore, in comparison with the perchlorate electrolyte with and without HA, an enhancement in degradation efficiency of 2.6 times was observed with HA injection. Hence, the effect of electrochemical nitrate reduction on BA removal was confirmed from the aforementioned observations.

To determine the effect of nitrates and the electrochemical behavior of HA, a separated electrochemical cell was introduced in which electrochemical activation of HA and enhancement of BA removal was observed at the anode. Moreover, the final product of the electrochemical activation of HA was confirmed as a nitrate. For identifying the reactive species during the electrochemical activation of HA, a scavenger test and electron spin resonance spectroscopy were conducted. It was discovered that the hydroxyl radical was the major oxidant species mediating the degradation of BA.

## Contents

Abstract.....	i
Contents .....	ii
List of Figures.....	iv
List of Tables.....	vi
Chapter 1. Introduction.....	1
I. Electrochemical pollutant removal .....	1
II. Potential of hydroxylamine (HA) for pollutants removal .....	2
Chapter 2. Materials and methods .....	3
I. Reagents .....	3
II. Experimental methods.....	3
III. Analytical methods .....	5
2.3.1 Electrolyte component analysis.....	5
2.3.2 Radical identification: electro spin resonance (ESR) spectroscopy.....	5
2.3.3 Electrochemical parameter .....	6
Chapter 3. Results and discussion .....	7
I. Nitrate reduction and hydroxylamine generation .....	7
3.1.1 Investigation of electrochemical condition for hydroxylamine generation.....	7
3.1.2 Comparison of various cathode material.....	9
II. Organic pollutants removal .....	13
3.2.1 Organic pollutants removal according to voltage .....	13
3.2.2 Efficiency comparison between system .....	16
3.2.3 Oxidation pathways .....	19
III. Identification of oxidant species.....	26
3.3.1 Scavenger test .....	26
3.3.2 ESR spectroscopy .....	27

<b>IV. Applicability of this study to wastewater treatment process .....</b>	<b>31</b>
<b>3.4.1 Application in various pH regions.....</b>	<b>31</b>
<b>3.4.2 Simultaneous removal of nitrate and organic pollutants .....</b>	<b>33</b>
<b>Chapter 4. Conclusions.....</b>	<b>35</b>
<b>References .....</b>	<b>37</b>



## List of Figures

Figure 1. Scheme of electrochemical nitrate reduction pathway .....	2
Figure 2. Photos of (a) electrochemical experimental set-up and (b) one-chambered cell .....	3
Figure 3. Scheme of two-compartment cell (a) without PEM and (b) with PEM. ....	4
Figure 4. (a) Electrochemical HA generation with time and (b) Faradaic efficiency and generation rate according to applied voltage .....	7
Figure 5. (a) Electrochemical HA generation with time and (b) Faradaic efficiency and generation rate according pH .....	8
Figure 6. (a) Concentration changes of nitrate with time, (b) final nitrate concentration and (c) nitrate conversion rate according to various cathode material during electrochemical reduction of nitrate.....	9
Figure 7. (a) Concentration changes of nitrite with time, (b) final nitrite concentration according to various cathode material during electrochemical reduction of nitrate.....	10
Figure 8. (a) Concentration changes of HA with time, (b) final HA concentration according to various cathode material during electrochemical reduction of nitrate .....	10
Figure 9. (a) Concentration changes of ammonium with time, (b) final ammonium concentration according to various cathode material during electrochemical reduction of nitrate.....	11
Figure 10. (a) Selectivity of nitrate reduction product by various electrodes, and (b) faradaic efficiency of hydroxylamine generation .....	11
Figure 11. (a) BA and (b) HA concentration changes during electrolysis of nitrate electrolyte...	13
Figure 12. (a) BA and (b) HA concentration changes during electrolysis of perchlorate electrolyte.....	14
Figure 13. (a) BA and (b) HA concentration changes during electrolysis of perchlorate with hydroxylamine electrolyte .....	15
Figure 14. BA removal rate according to applied voltage with various electrolytes.....	16
Figure 15. BA removal efficiency according to applied voltage with various electrolytes.....	17
Figure 16. BA removal efficiency according to average current density with various electrolytes .....	18
Figure 17. BA removal by electrolysis in two-chambered reactor (a) without PEM and (b) with PEM.....	19

<b>Figure 18. Concentration changes of N-species during hydroxylamine electrolysis in two-chambered reactor .....</b>	<b>20</b>
<b>Figure 19. BA degradation by hydroxylamine/hydrogen peroxide upon various electrolytes .....</b>	<b>22</b>
<b>Figure 20. BA degradation by metal/hydroxylamine/hydrogen peroxide .....</b>	<b>22</b>
<b>Figure 21. BA degradation by peroxynitrite .....</b>	<b>25</b>
<b>Figure 22. Effect of DMSO on various electrolytes during electrolysis .....</b>	<b>26</b>
<b>Figure 23. ESR spectra obtained by spin trapping with DMPO during electrolysis .....</b>	<b>27</b>
<b>Figure 24. ESR signals of DMPO spin trapping adducts produced by peroxynitrite .....</b>	<b>28</b>
<b>Figure 25. (a) ESR intensity obtained by spin trapping with DMPO during electrolysis and (b) initial part of result .....</b>	<b>28</b>
<b>Figure 26. ESR intensity according to current density .....</b>	<b>29</b>
<b>Figure 27. BA degradation by electrolysis of perchlorate electrolyte at (a) pH 1.5, (b) 7.0, and (c) 12.5 .....</b>	<b>31</b>
<b>Figure 28. BA degradation by electrolysis of nitrate electrolyte at (a) pH 1.5, (b) 7.0, and (c) 12.5 .....</b>	<b>31</b>
<b>Figure 29. BA degradation by electrolysis of HA added perchlorate electrolyte at (a) pH 1.5, (b) 7.0, and (c) 12.5 .....</b>	<b>32</b>
<b>Figure 30. Simultaneous removal of nitrate and organic pollutants during nitrate reduction process .....</b>	<b>33</b>
<b>Figure 31. Scheme of electrochemical removal of nitrate and organic pollutant .....</b>	<b>35</b>

## List of Tables

Table 1. Various oxidants electrochemically produced from wastewater component.....	1
Table 2. Oxidation state of nitrogen species.....	2

## Chapter 1. Introduction

### I. Electrochemical pollutant removal

In many water sources, concerns have been raised about refractory organic pollutants due to their detrimental effects on humans and the environment. Various methods have been developed in different engineering fields involving chemical, biological, physical, and electrochemical disciplines. Among them, electrochemical processes are receiving increasing attention because they are environmentally benign,<sup>1</sup> convenient for combining with other technologies, and generally require no auxiliary chemicals.<sup>2</sup>

An electrochemical process removes contaminants through direct electron transfer by the electrodes (direct oxidation), but it can also remove contaminants by using various molecules in water (indirect oxidation), during which it uses a variety of components in the water such as ions (chlorides, sulfates, and ETCs), dissolved oxygen, and water molecules (Table 1). The process makes those molecules reactive, thereby becoming like oxidants or radicals capable of degrading refractory organic pollutants. Therefore, the proper selection of electrodes for utilizing wastewater components and electrical conditions (current density or voltage) enables the achieving of high pollutant removal and cost efficiency.

**Table 1.** Various oxidants electrochemically produced from wastewater component.

Wastewater component	Oxidant	E° (V/NHE)	Generation reaction	Applicable electrode
Water molecule	Hydroxyl radical	1.89 <sup>3</sup> - 2.80 <sup>3</sup>	$\text{H}_2\text{O} \rightarrow \cdot\text{OH} + \text{H}^+ + \text{e}^-$	BDD, PbO <sub>2</sub>
	Hydrogen peroxide	0.88 <sup>3</sup> - 1.45 <sup>3</sup>	$2\text{H}_2\text{O} \rightarrow \text{H}_2\text{O}_2 + 2\text{H}^+ + 2\text{e}^-$	BVO <sub>4</sub>
	Ozone	1.24 <sup>3</sup> - 2.08 <sup>3</sup>	$3\text{H}_2\text{O} \rightarrow \text{O}_3 + 6\text{H}^+ + 6\text{e}^-$	PbO <sub>2</sub>
Oxygen molecule	Hydrogen peroxide	0.88 <sup>3</sup> - 1.45 <sup>3</sup>	$\text{O}_2 + 2\text{H}^+ + 2\text{e}^- \rightarrow \text{H}_2\text{O}_2$	GDE, Carbonaceous material
Sulfate ion	Sulfate radical	2.50 <sup>4</sup> - 3.10 <sup>4</sup>	[direct] $\text{SO}_4^{2-} \rightarrow \text{SO}_4^{\cdot-} + \text{e}^-$ [indirect] $\text{SO}_4^{2-} + \cdot\text{OH} \rightarrow \text{SO}_4^{\cdot-} + \text{OH}^-$	BDD, PbO <sub>2</sub> , Pt
	Peroxydisulfate	2.01 <sup>5</sup> - 2.12 <sup>5</sup>	$2\text{SO}_4^{\cdot-} \rightarrow \text{S}_2\text{O}_8^{2-}$	
	Peroxymonosulfate	1.22 <sup>6</sup> - 1.81 <sup>6</sup>	$\text{S}_2\text{O}_8^{2-} + \text{H}_2\text{O} \rightarrow \text{HSO}_5^- + \text{HSO}_4^-$	
Chloride ion	Chlorine	1.36 <sup>5</sup>	$2\text{Cl}^- \rightarrow \text{Cl}_2 + 2\text{e}^-$	IrO <sub>2</sub> , RuO <sub>2</sub>
	Hypochlorite	0.84 <sup>3</sup> - 1.48 <sup>3</sup>	$\text{Cl}_2 + \text{H}_2\text{O} \rightarrow \text{HOCl} + \text{H}^+ + \text{Cl}^-$	

## II. The potential of hydroxylamine (HA) for pollutant removal

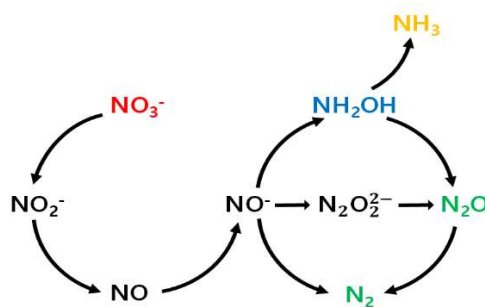


**Figure 1.** Scheme of electrochemical nitrate reduction pathway

Among the various wastewater components, there are a considerable number of wastewater cases, including nitrates.<sup>7–10</sup> The electrochemical reduction of nitrates and HA generation pathway have been reported by Kastsounaros (Figure 1).<sup>11,12</sup> In addition, various electrochemical reactions of HA have been reported.<sup>13–20</sup> However, there has been little research into using nitrate ions to produce reactive oxidants. So far, most studies on the nitrate electrochemical process have been aimed at converting nitrate into nitrogen gas (Figure 1).<sup>21</sup> During the process, various kinds of intermediates are produced such as nitrites, HA, nitrous oxide, nitrogen oxide species, and ETCs (Table 2). It can be postulated that some of these intermediates can react directly with organic compounds or be converted into reactive species capable of degrading organic compounds.

**Table 2.** Oxidation state of nitrogen species

Oxidation state	Chemical formula	Name	Oxidation state	Chemical formula	Name
5	$\text{NO}_3^-$	Nitrate	0	$\text{N}_2$	Dinitrogen
4	$\text{N}_2\text{O}_4$	Dinitrogen tetroxide	-0.33	$\text{HN}_3$	Hydrazoic acid
3	$\text{NO}_2^-$	Nitrite	-1	$\text{NH}_2\text{OH}$	Hydroxylamine
2	$\text{NO}$	Nitric oxide	-2	$\text{N}_2\text{H}_4$	Hydrazine
1	$\text{H}_2\text{N}_2\text{O}_2$	Nitramide	-3	$\text{NH}_3$	Ammonia
	$\text{N}_2\text{O}_3^{2-}$	Hyponitrate			
	$\text{N}_2\text{O}$	Nitrous oxide			

In practice, HA (one of the intermediates) can be used as an iron (or copper (Cu))-reducing agent to accelerate Fenton (-like) reactions for the degradation of organic compounds and the inactivation of microorganisms.<sup>22–29</sup> Moreover, it can act as a reagent to produce an oxidizing agent (such as hydroxyl,<sup>30,31</sup> sulfate,<sup>32</sup> superoxide,<sup>33</sup> and amino radicals,<sup>34</sup> as well as peroxyxynitrite<sup>35</sup>). Nevertheless, there have been insufficient studies on the electrochemical application of HA to water/wastewater treatment processes. Therefore, the proper use of intermediates produced during the electrochemical nitrate reduction process can simultaneously allow the control of nitrate and refractory organic contaminants in wastewater.

## Chapter 2. Materials and methods

### I. Reagents

All chemicals were of reagent grade and used without further purification: nitric acid ( $\text{HNO}_3$ ), perchloric acid ( $\text{HClO}_4$ ), benzoic acid (BA), HA, sodium nitrite ( $\text{NaNO}_2$ ), ammonium hydroxide, urea, 8-hydroxyquinolinol, sodium carbonate, methanol, t-butanol, phosphoric acid, sodium hydroxide ( $\text{NaOH}$ ), methanesulfonic acid (MSA), hydrogen peroxide ( $\text{H}_2\text{O}_2$ ), hydrochloric acid ( $\text{HCl}$ ), manganese dioxide, dimethyl sulfoxide (DMSO), 5,5-dimethyl-1-pyrroline N-oxide (DMPO) (all purchased from Sigma-Aldrich Co.), and acetonitrile (J. T. Baker Co.). All solutions were prepared using 18.2  $\text{M}\Omega\cdot\text{cm}$  Milli-Q water from a Millipore system (Millipore Co.). Stock solutions of BA (10 mM),  $\text{HNO}_3$  (1 M),  $\text{HClO}_4$  (1 M),  $\text{HCl}$  (0.6 M),  $\text{NaOH}$  (1.5 M) were prepared and stored at 4 °C until used. HA (0.5 M),  $\text{H}_2\text{O}_2$  (0.7 M and 100 mM), and  $\text{NaNO}_2$  (0.6 M) were prepared prior to the experiments.

### II. Experimental methods

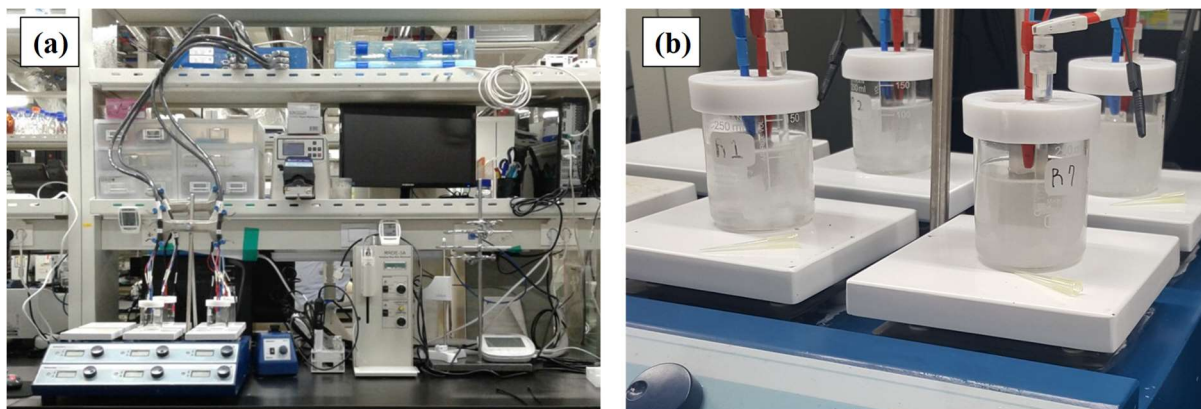


**Figure 2.** Photos of (a) electrochemical experimental set-up and (b) one-chambered cell

Platinum (Pt) foil (Alfa Aesar Co.) was used as the anode whereas Cu, silver (Ag), stainless steel (SS), titanium (Ti), aluminum (Al), nickel (Ni), and zinc (Zn) foil (Sigma-Aldrich Co.) and tin (Sn) plate (Alfa Aesar Co.) were used as the cathode. All of the electrode materials were prepared by cutting into a  $2.5 \times 2.5 \text{ cm}^2$  square. The immersed areas of the anode and cathode in an electrolyte solution

were the equivalent of 10 cm<sup>2</sup> of effective electrode area. Voltage was controlled via a three-electrode configuration using a saturated calomel electrode (SCE) with a multichannel potentiostat (VSP, BioLogic Science Instruments) and electrochemical measurements were recorded using EC-Laboratory version 11.10 (BioLogic Science Instruments) installed on a computer-interfaced system.

One- and two-compartment cells were constructed: a top-cut glass beaker was used as the one-compartment cell (Figure. 2) and a customized Teflon cell as the two-compartment cell, with which separate observations of the anodic and cathodic reactions were possible (Figure 3). The two-compartment cell was separated by a proton-exchange membrane (PEM; Nafion 117, Dupont). Some experiments were conducted without a PEM in the two-compartment cell. The volume of electrolyte solution in each compartment was 100 mL and the electrochemical reaction started with the application of specified potential (or current). 1.5 mL of sample was drawn for further analysis at designated time intervals.

BA was used as a refractory organic pollutant. Nitric and perchloric acid solutions were prepared as an electrolyte (or supporting electrolyte). Peroxynitrite (ONOOH) was prepared daily just prior to use via the reaction of nitrite and H<sub>2</sub>O<sub>2</sub> with a slight modification to Robinson and Beckman's method.<sup>36</sup>

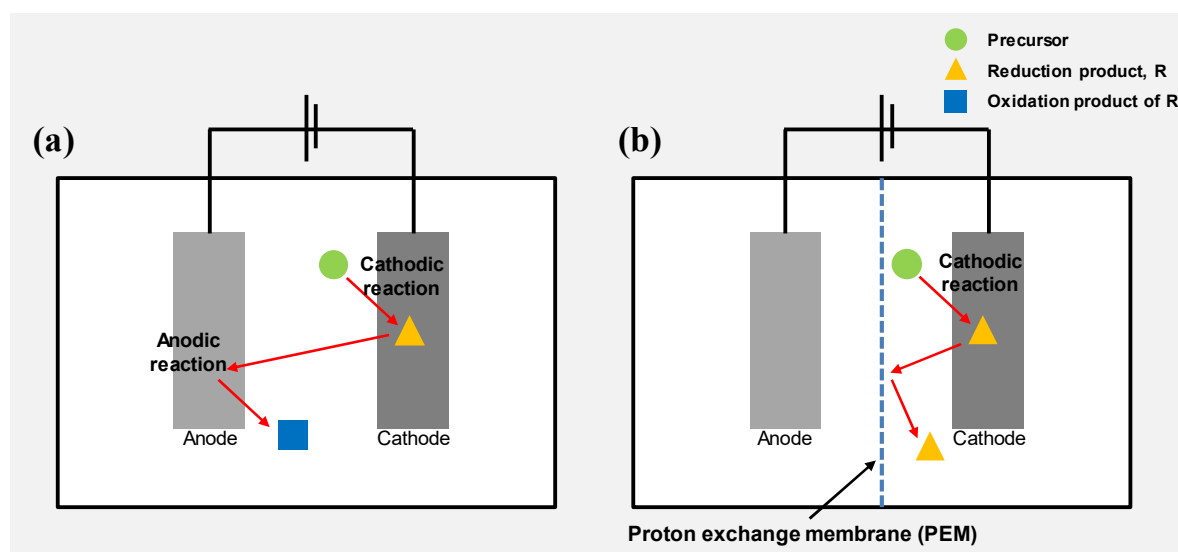


**Figure 3.** Scheme of two-compartment cell (a) without PEM and (b) with PEM.

### III. Analytical methods

#### 2.3.1 Electrolyte component analysis

Nitrate and nitrite levels were determined via an ICS-2100 ion chromatography system (Thermo Fisher Scientific Inc.) equipped with an AERS 500 electrolytically regenerated suppressor (Dionex Co.), conductivity detector and a potassium hydroxide eluent generator cartridge (EGC III KOH, Dionex Co.). Separation was performed on a Dionex IonPac AS-16 anionic column using 22 mM of potassium hydroxide solution as the mobile phase at a flow rate of 1 mL/min. Ammonia was determined via an ICS-1600 ion chromatography system (Thermo Fisher Scientific Inc.) equipped with a CERS 500 electrolytically regenerated suppressor (Dionex Co.) and conductivity detector. Separation was performed on a Dionex IonPac CS-17 cationic column using 6 mM of MSA solution as the mobile phase at a flow rate of 1 mL/min.

The concentrations HA in solution was determined using 8-hydroxyquinolinol and the concentration of the ONOOH stock solution was determined directly at 302 nm (absorbance coefficient =  $1670 \text{ M}^{-1} \text{ cm}^{-1}$ ) via UV-Vis spectroscopy (Lambda 465, PerkinElmer Co.).<sup>36,37</sup> BA was analyzed using an Ultimate™ 3000 high-performance liquid chromatography system (Thermo Fisher Scientific Inc.) with UV absorbance detection at 227 nm. Separation was performed on a Dionex Acclaim C-18 column (250 x 4.6 mm, 5  $\mu\text{m}$ ) using a binary mixture of phosphoric acid (0.1 % v/v) and acetonitrile was used as the mobile phase at a flow rate of 1 mL/min. The concentrations of total organic carbon (TOC) and total nitrogen (TN) were determined using a TOC/TN analyzer (TOC-V<sub>CPH</sub> with a TN module, Shimadzu Co.).

#### 2.3.2 Radical identification via electron spin resonance (ESR) spectroscopy

An ESR spectrometer (JES-X310, Jeol Co.) was used to qualify radical species with 10 mM of DMPO as the spin-trapping agent. Samples were collected from the electrochemical reactor and transferred to a flat quartz cell for the ESR analysis. ESR signals of the DMPO-radical spin-adduct obtained during the electrolysis were measured with a 9.42 GHz microwave (1.00 mW) at a modulation frequency of 100 kHz and a modulation amplitude of 2.0 G.



### 2.3.3 Electrochemical parameters

The performances of the cathode materials are presented as the selectivity, nitrate conversion rate, and Faradaic efficiency:

$$\text{Selectivity (\%)} = \frac{\Delta[\text{Product}]}{\Delta[\text{Nitrate}]} \times 100, \quad (1)$$

$$\text{Nitrate conversion rate (mmol/m}^2\text{/h)} = \frac{\Delta[\text{Nitrate}]}{t \times S}, \quad (2)$$

$$\text{Faradaic efficiency of HA (\%)} = \frac{6 \times F \times \Delta[\text{HA}]}{\int_0^t I(t) dt} \times 100. \quad (3)$$

In addition, the coulombic efficiency and the average current density of BA were calculated to compare its decomposition efficiency according to the voltage and the electrolytes using the following equations:

$$\text{Coulombic efficiency of BA removal (\%)} = \frac{\Delta[\text{BA}]}{\int_0^t I(t) dt} \times 100, \quad (4)$$

$$\text{Average current density (mA/cm}^2\text{)} = \frac{\int_0^t I(t) dt}{t \times S}. \quad (5)$$

In Equations (1-5),  $\Delta[\text{Product}]$ ,  $\Delta[\text{Nitrate}]$ ,  $\Delta[\text{HA}]$ , and  $\Delta[\text{BA}]$  stand for the difference in molecular concentration between the initial time and specific electrolysis time,  $t$  (the products were nitrite, HA, and ammonium ions),  $S$  is effective electrode area (in this study,  $S = 10 \text{ cm}^2$ ),  $I(t)$  is the electrolysis current at time  $t$ . The moles of consumed electrons during electrolysis (coulomb) is calculated from  $\int_0^t I(t) dt$ ; e.g. a value of 6 would mean that the 6 moles of electrons are needed for the formation of 1 mole of HA from nitrates (in acidic media,  $\text{NO}_3^- + 8\text{H}^+ + 6\text{e}^- \rightarrow \text{NH}_3\text{OH}^+ + 2\text{H}_2\text{O}$ ).  $F$  is the Faraday constant ( $96,485 \text{ A}\cdot\text{sec/mol}$ ).

## Chapter 3. Results and discussion

### I. Nitrate reduction and HA generation

#### 3.1.1 Investigation of the electrochemical conditions for HA generation

Prior to a comparison of the performance of the various electrodes, the influence of initial pH and the applied voltage were investigated with Sn since it is already known to exhibit high selectivity for HA.<sup>38</sup>

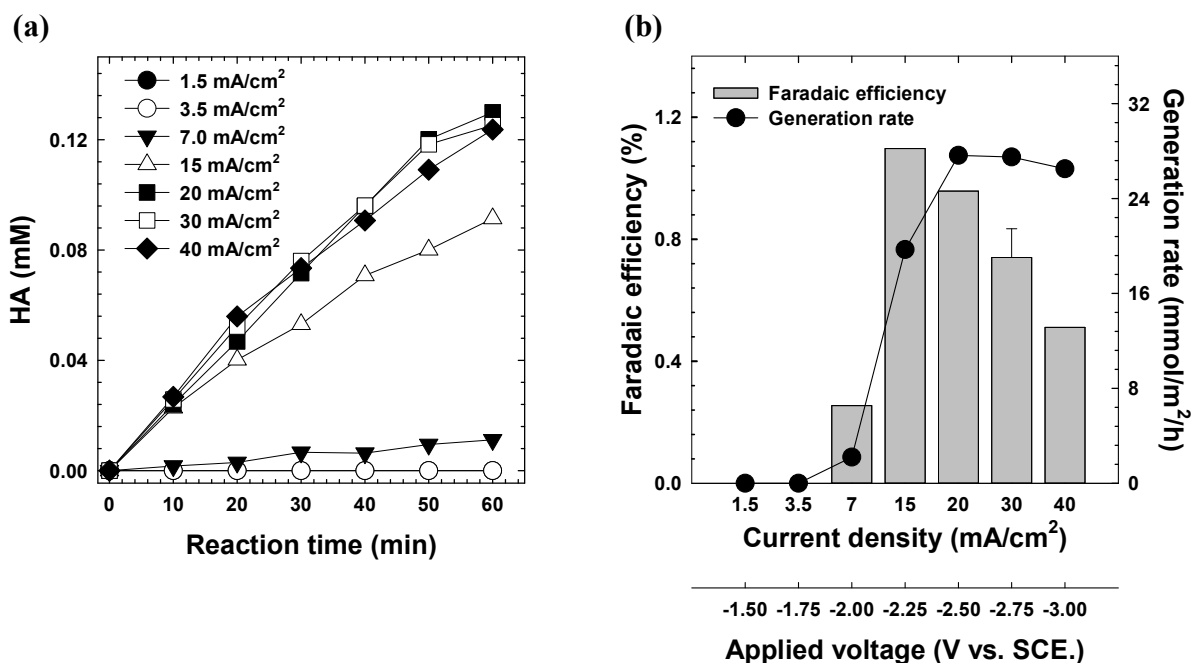


**Figure 4.** (a) Electrochemical HA generation with time and (b) Faradaic efficiency and generation rate according to applied voltage (Working electrode = Sn plate, Counter electrode = Platinum foil, Reference electrode = Saturated Calomel Electrode, Effective electrode area = 10 cm<sup>2</sup>, [Nitrate]<sub>0</sub> = 0.05 M, pH<sub>i</sub> = 7.0, Faradaic efficiency and generation rate were calculated with 60 minutes data).

For current density, a higher value generated the more HA (Figure 4). The generation of HA was observable from 7 mA/cm<sup>2</sup> and started to become saturated at 20 mA/cm<sup>2</sup>. However, Faradaic efficiency (which shows electrical efficiency) increased up to 15 mA/cm<sup>2</sup> and then decreased. The highest final production of HA was 0.129 mM at 20 mA/cm<sup>2</sup>, with a Faradaic efficiency of 0.96% and the highest

production rate of 27.64 mmol/m<sup>2</sup>/h. Meanwhile, the highest Faradaic efficiency (1.10%) appeared at 15 mA/cm<sup>2</sup>, at which the amount of HA produced was 0.091 mM during 1 hour of electrolysis at a production rate of 19.70 mmol/m<sup>2</sup>/h. It was considered that sufficient electrons had been supplied for the generation of HA at 30 mA/cm<sup>2</sup>, and so this was selected as the experimental current density to investigate the effect of pH on HA generation by the Sn cathode.

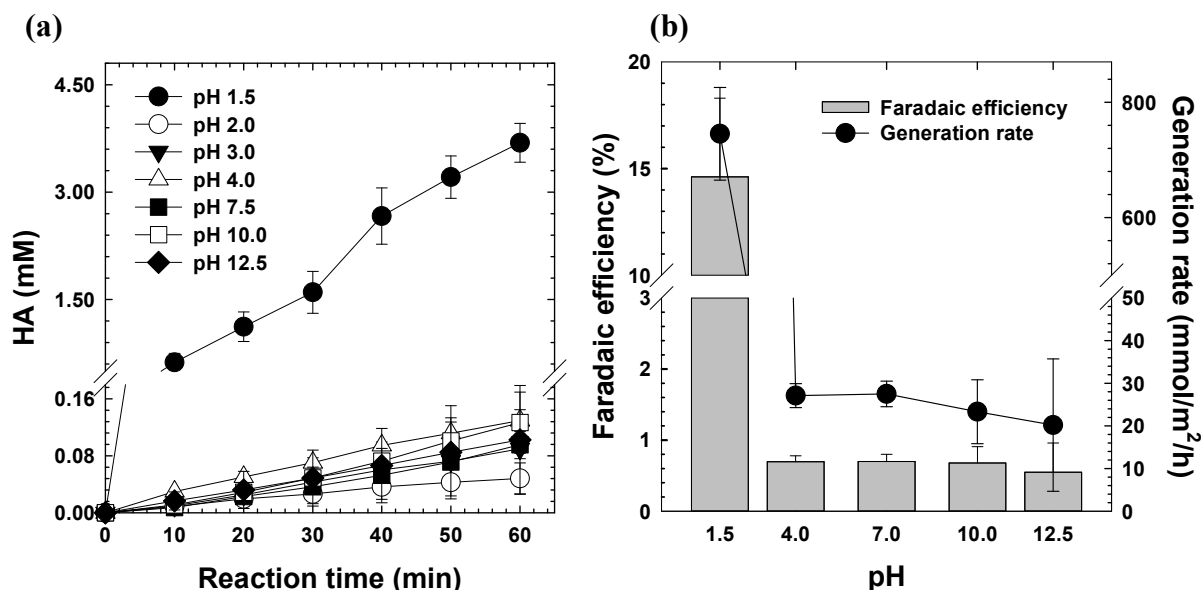


**Figure 5.** (a) Electrochemical HA generation with time and (b) Faradaic efficiency and generation rate according pH (Cathode = Sn plate, Anode = Platinum foil, Effective electrode area = 10 cm<sup>2</sup>, [Nitrate]<sub>0</sub> = 0.05 M; pH<sub>i</sub> = 7.0, Applied current = 30 mA/cm<sup>2</sup>, Faradaic efficiency and generation rate were calculated with 60 minutes data)

A lower pH generated more HA (Figure 5), and at over pH 2.0, the generation of HA was poor. However, HA generation drastically increased at pH 1.5. The final concentration of HA was 3.69 mM with 14.62% Faradaic efficiency and a production rate of 745.35 mmol/m<sup>2</sup>/h. Since it is essential to supply sufficient hydrogen ions for HA generation,<sup>38</sup> the initial pH of the electrolyte was set at 1.3 (the natural pH of 0.05 M nitric acid and perchloric acid) and the current density was set at 30 mA/cm<sup>2</sup>. Under these conditions, nitrate reduction experiments were conducted with the various cathode materials.

### 3.1.2 Comparison of the various cathode materials

Since the nitrate reduction reaction takes place at potentials where the hydrogen evolution reaction occurs in parallel, voltammetric measurements cannot provide reliable information on the reduction of nitrate and the generation of HA. Therefore, the selectivity of products, nitrate conversion rate, and Faradaic efficiency were measured as cathode performance parameters for electrochemical HA generation.<sup>38</sup>

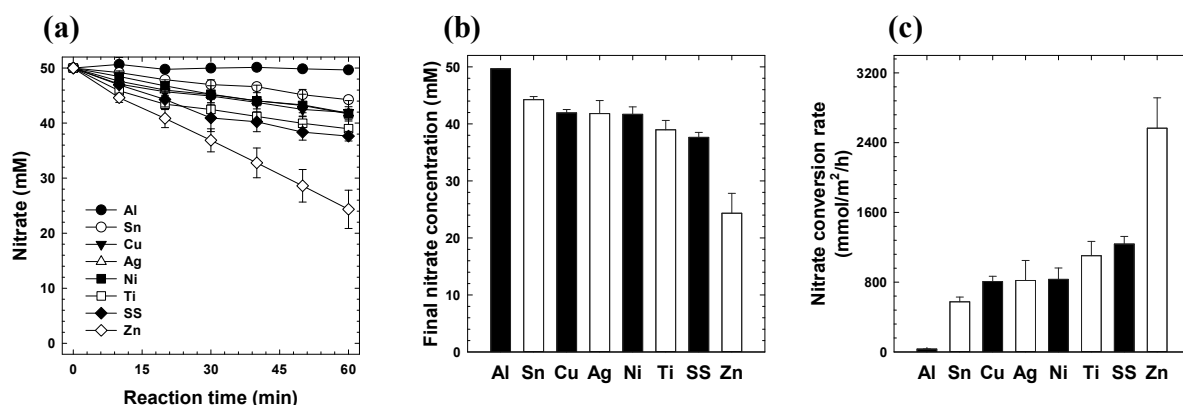


**Figure 6.** (a) Concentration changes of nitrate with time, (b) final nitrate concentration and (c) nitrate conversion rate according to various cathode material during electrochemical reduction of nitrate (Anode = platinum foil, effective electrode area = 10 cm<sup>2</sup>, [Nitrate]<sub>0</sub> = 0.05 M, pH<sub>i</sub> = 1.3, current density = 30 mA/cm<sup>2</sup>)

The nitrate concentration was reduced during the electrolysis with the various cathode materials (Figure 6). The highest nitrate reduction was found with Zn, while Al converted the smallest. The concentration of nitrate remaining after 1 hour of electrolysis was 49.67, 44.25, 41.93, 41.81, 41.68, 38.97, 37.63, and 24.34 mM for Al, Sn, Cu, Ag, Ni, Ti, SS, and Zn, respectively. As a result, the highest conversion rate of nitrate was found to be Zn at 2,566.45 mmol/m<sup>2</sup>/h.

Decreased nitrate should have been converted to another form by the electrochemical reaction, and so nitrite and ammonia were measured since they are relatively stable intermediates in aqueous solution, and the target product HA was also measured, as depicted in Figures 7–9, respectively.

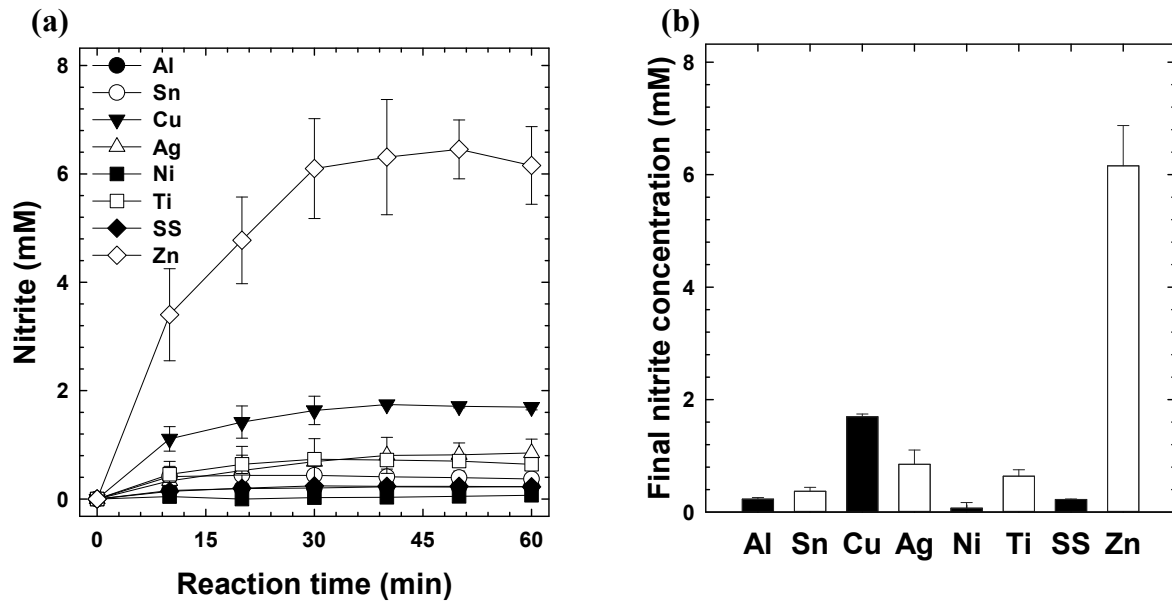


**Figure 7.** (a) Concentration changes of nitrite with time, (b) final nitrite concentration according to various cathode material during electrochemical reduction of nitrate (Anode = platinum foil, effective electrode area = 10 cm<sup>2</sup>, [Nitrate]<sub>0</sub> = 0.05 M, pH<sub>i</sub> = 1.3, current density = 30 mA/cm<sup>2</sup>)

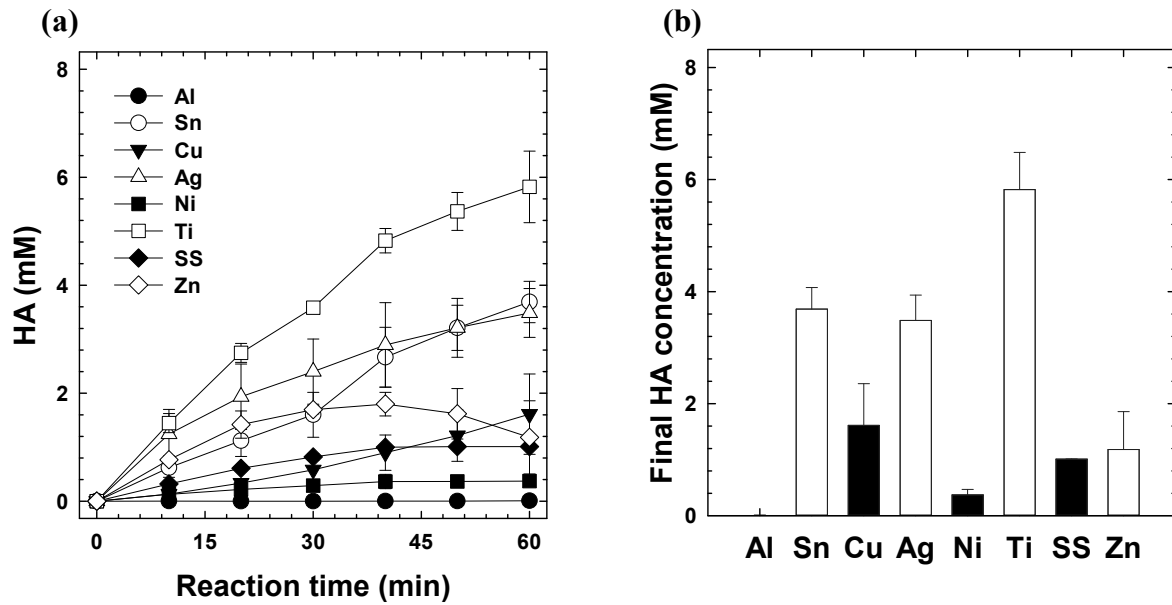


**Figure 8.** (a) Concentration changes of HA with time, (b) final HA concentration according to various cathode material during electrochemical reduction of nitrate (Anode = platinum foil, effective electrode area = 10 cm<sup>2</sup>, [Nitrate]<sub>0</sub> = 0.05 M, pH<sub>i</sub> = 1.3, current density = 30 mA/cm<sup>2</sup>)

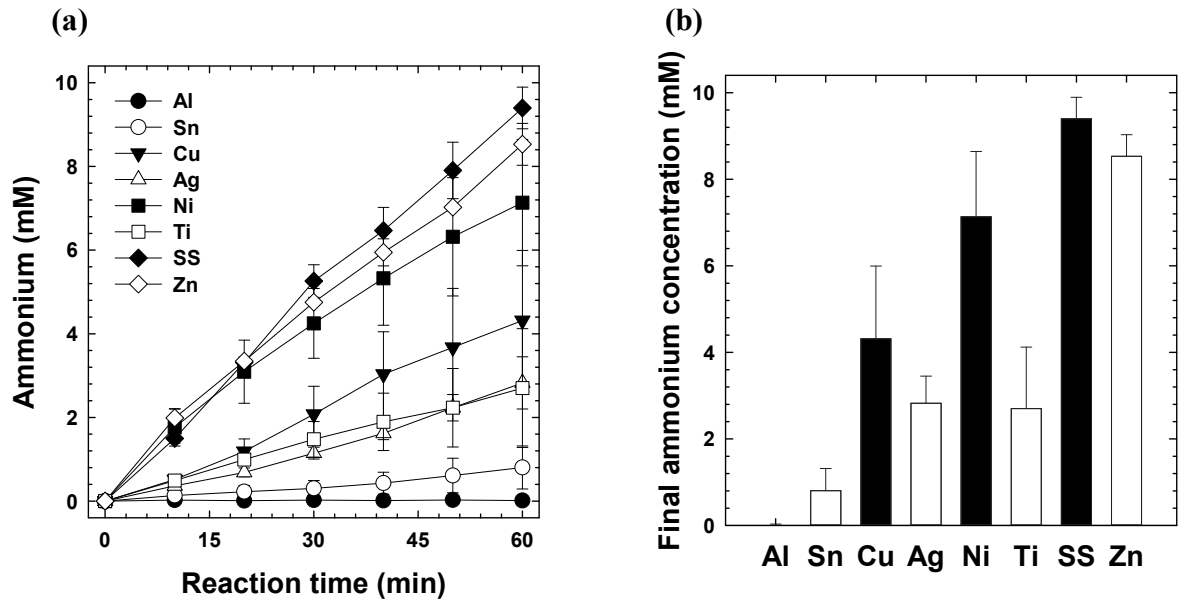


**Figure 9.** (a) Concentration changes of ammonium with time, (b) final ammonium concentration according to various cathode material during electrochemical reduction of nitrate (Anode = platinum foil, effective electrode area = 10 cm<sup>2</sup>, [Nitrate]<sub>0</sub> = 0.05 M, pH<sub>i</sub> = 1.3, current density = 30 mA/cm<sup>2</sup>)

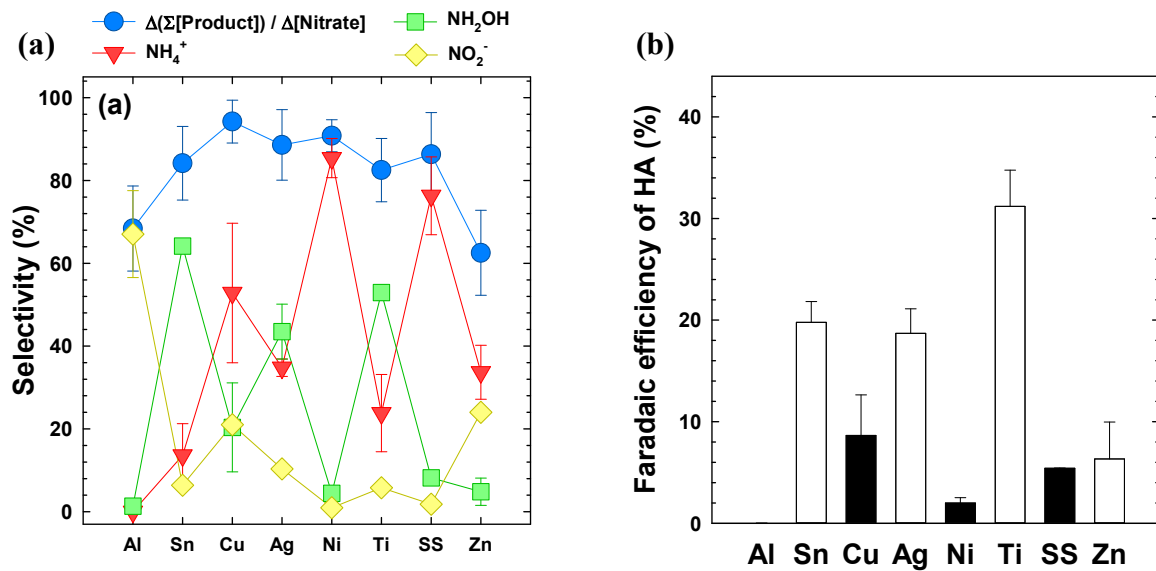


**Figure 10.** (a) Selectivity of nitrate reduction product by various electrodes, and (b) faradaic efficiency of hydroxylamine generation (Anode = platinum foil, effective electrode area = 10 cm<sup>2</sup>, current density = 30 mA/cm<sup>2</sup>, pH<sub>i</sub> = 1.3, [Nitrate]<sub>0</sub> = 0.05 M, the selectivity was calculated after 1 hour of electrolysis).

In the case of nitrite generation, Zn achieved the highest final concentration of 6.16 mM, followed by Cu at 1.70 mM; the other electrodes produced negligible amounts of nitrite. In the case of HA, Ti produced the largest amount at 5.82 mM, followed by Sn and Ag at 3.69 and 3.49 mM respectively. The highest production of ammonia was observed at the SS electrode (9.40 mM), while Zn, Ni, and Cu produced 8.53, 7.13, and 4.32 mM, respectively.

The calculated performance parameters for selectivity and Faradaic efficiency of HA production are shown in Figure 10. The results of selectivity were compared for the electrode materials in the aspect of nitrate conversion ability. Al attained significantly higher selectivity for nitrite (67.06%), while the other materials were less than 25%. Sn and Ti achieved high selectivity for HA (64.16 and 52.91%, respectively), while Ni and SS showed high selectivity for ammonia (85.41 and 76.31%, respectively).

However, the tendency of the nitrate conversion rate was not the same as that for HA selectivity. Zn acquired the highest nitrate conversion rate, followed by SS and Ti, resulting in different generated amounts and Faradaic efficiencies of HA. The highest amount of HA appeared at the Ti electrode, as shown in Figure 8. Under constant current conditions, the Faradaic efficiency of HA should have been in the same order as the generation of HA. The Faradaic efficiency of HA generation was 31.20, 19.78, 18.69, 6.64, 6.34, 5.42, 2.00, and 0.02% for Ti, Sn, Ag, Cu, Zn, SS, Ni, and Al, respectively.

It was found that Ti was the most charge-efficient material for HA generation (31% Faradaic efficiency for HA), which is 1.6 times higher than Sn with the highest selectivity of HA and 4.9 times higher than Zn with the highest nitrate conversion rate. As a result, Ti was chosen as the optimum electrode for electrochemical HA generation.

## II. Organic pollutant removal

To explore the effect of HA produced during the electrochemical nitrate reduction process, electrolysis experiments were conducted with BA as the refractory organic pollutant with nitrate, perchlorate, and perchlorate with HA electrolytes (Figures 11–13, respectively). Furthermore, the decomposition rate of BA according to the applied voltage and the BA removal efficiency according to average current density are depicted in Figures 14–16, respectively.

### 3.2.1 Organic pollutant removal according to voltage

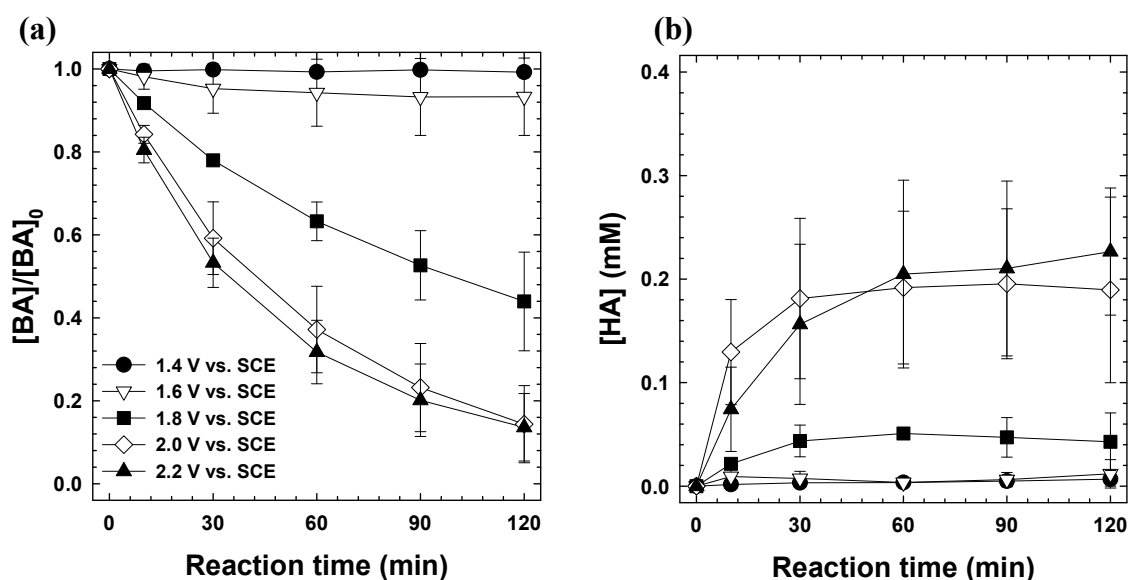


**Figure 11.** (a) BA and (b) HA concentration changes during electrolysis of nitrate electrolyte (Working electrode = platinum foil, counter electrode = titanium foil, reference electrode = saturated calomel electrode, effective electrode area = 10 cm<sup>2</sup>, pH<sub>i</sub> = 1.3, [Nitrate]<sub>0</sub> = 0.05 M, [Hydroxylamine]<sub>0</sub> = 5.0 mM, [Benzoic acid]<sub>0</sub> = 0.1 mM).

With the nitrate electrolyte, BA removal efficiency significantly increased from 1.8 V vs. SCE; as much as 56% removal was achieved in 2 hours (Figure. 11). At the same time, the accumulation of HA (approximately 0.04 mM) was observed with the BA degradation. In contrast, the BA removal was minor and HA accumulation was negligible at 1.6 V vs. SCE. At 2.0 and 2.2 V vs. SCE, the removal efficiency significantly increased again (85% in 2 hours). The accumulation of HA also significantly increased; its maximum accumulated concentration was 0.23 mM in 2 hours.



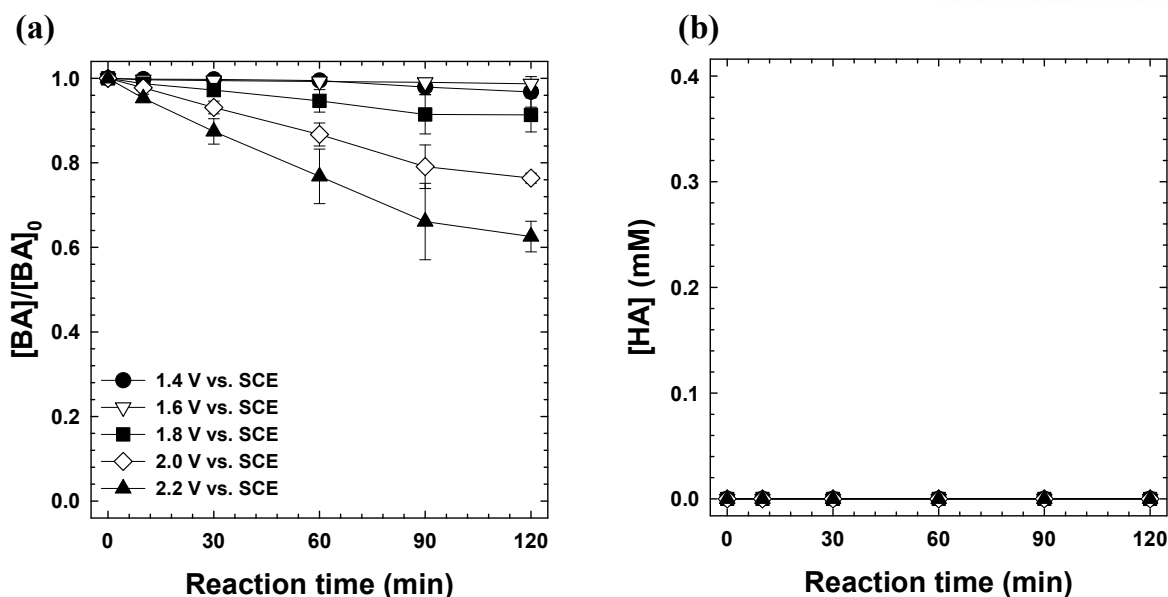


**Figure 12.** (a) BA and (b) HA concentration changes during electrolysis of perchlorate electrolyte (Working electrode = platinum foil, counter electrode = titanium foil, reference electrode = saturated calomel electrode, effective electrode area = 10 cm<sup>2</sup>, pH<sub>i</sub> = 1.3, [Perchlorate]<sub>0</sub> = 0.05 M, [Hydroxylamine]<sub>0</sub> = 5.0 mM, [Benzoic acid]<sub>0</sub> = 0.1 mM).

To confirm whether the electrochemical reduction of nitrate affected decomposition of BA, perchlorate, known as an inert electrolyte, was selected as the control experiment (Figure 12). At 1.4 and 1.6 V vs. SCE, BA removal was minor whereas from 1.8 V vs. SCE, BA removal was 9%. In addition, the maximum removal rate was 37% at 2.2 V vs. SCE in 2 hours. According to Montilla et al.,<sup>39</sup> the oxidation of BA starts from 1.8 V vs. ESS ( $\approx$  1.40 V vs. SCE), which is consistent with the results of the present study.

The major oxidation pathway of BA in the perchlorate electrolyte is considered to be the direct oxidation at the anode. Other oxidation pathways including hydroxyl radicals or H<sub>2</sub>O<sub>2</sub> could also exist in this electrolyte but their effects were minor (the details are discussed later).

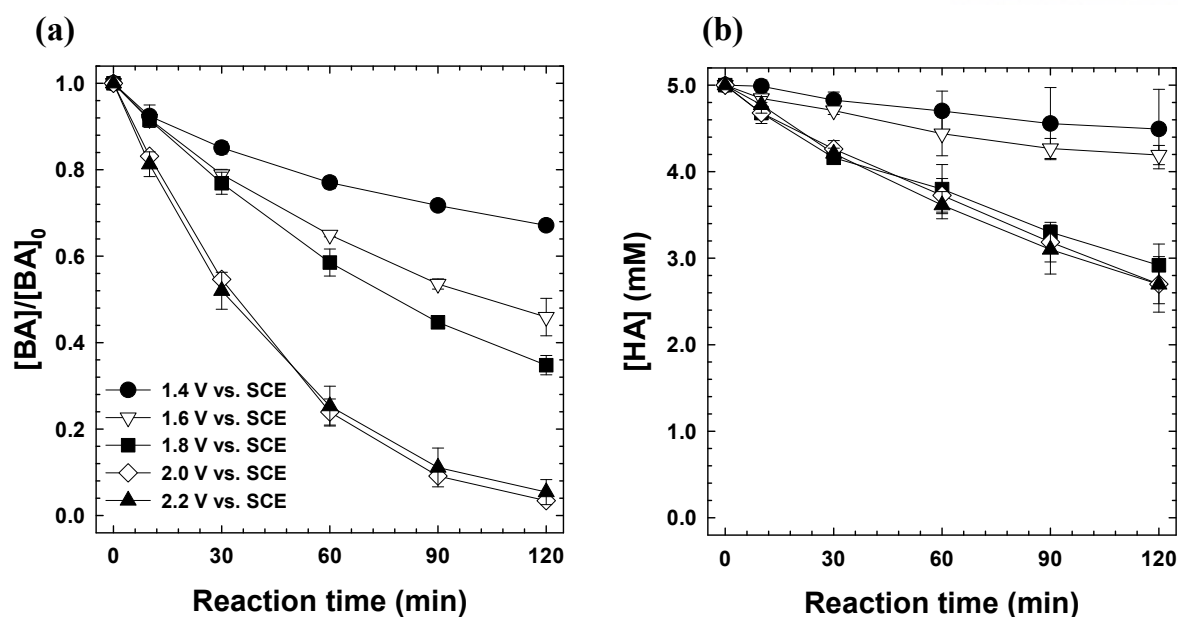
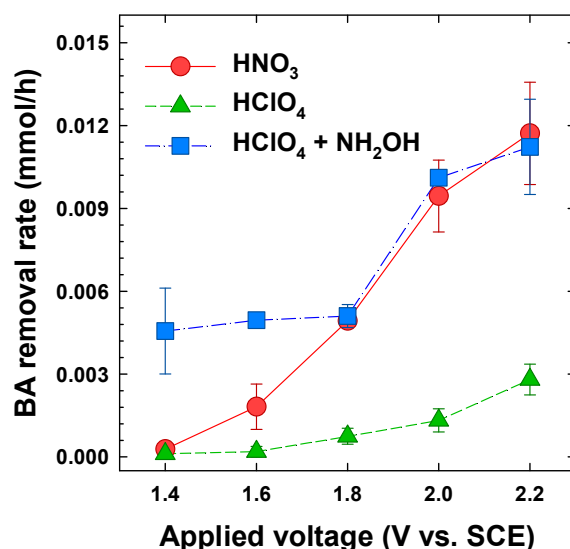


**Figure 13.** (a) BA and (b) HA concentration changes during electrolysis of perchlorate with hydroxylamine electrolyte (Working electrode = platinum foil, counter electrode = titanium foil, reference electrode = saturated calomel electrode, effective electrode area = 10 cm<sup>2</sup>, pH<sub>i</sub> = 1.3, [Perchlorate]<sub>0</sub> = 0.05 M, [Hydroxylamine]<sub>0</sub> = 5.0 mM, [Benzoic acid]<sub>0</sub> = 0.1 mM).

Perchlorate with injected HA electrolyte was investigated to prove the effect of HA (Figure 13). BA removal was observed from 1.4 V vs. SCE (33%), which is a rather encouraging result as the other electrolytes did not show a significant removal of BA at 1.4 V vs. SCE. At the same time, HA degradation was observed by as much as 0.5 mM. Although the experiments were conducted at 1.4 V vs. SCE and no results were presented below 1.4 V vs. SCE, it is known that HA degradation by oxidation starts from approximately 0.7 V vs. SCE according to previous studies.<sup>16</sup> Indeed, as the voltage increased, the removal efficiency of and the degradation of HA also increased. From 2.0 V vs. SCE, the removal rate seemed to be saturated at ~95%, and 2.0 V and 2.2 V vs. SCE showed a similar BA removal tendency.

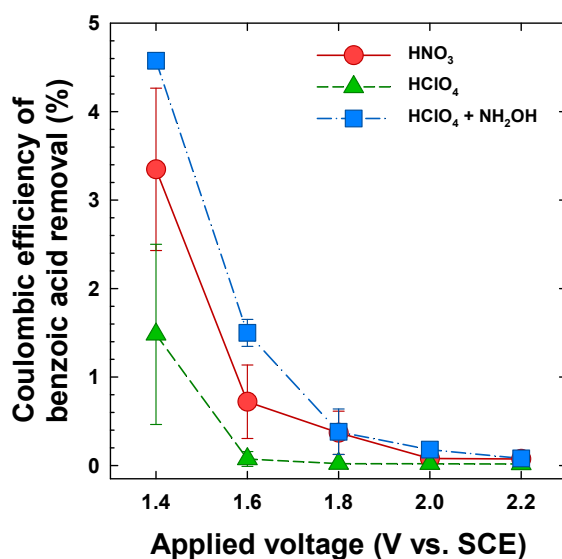
### 3.2.2 Efficiency comparison between the systems

From 1.8 V vs. SCE, the voltage indicated for HA accumulation during electrolysis, the nitrate electrolyte condition showed a similar trend of BA removal to perchlorate with HA. This result indicates that HA had a definite effect on BA degradation. To ensure this effect, we compared the BA removal rate and coulombic efficiency of BA removal according to applied voltage (Figures 14–15). Furthermore, energy consumption with the three electrolytes was also compared (Figure 16).



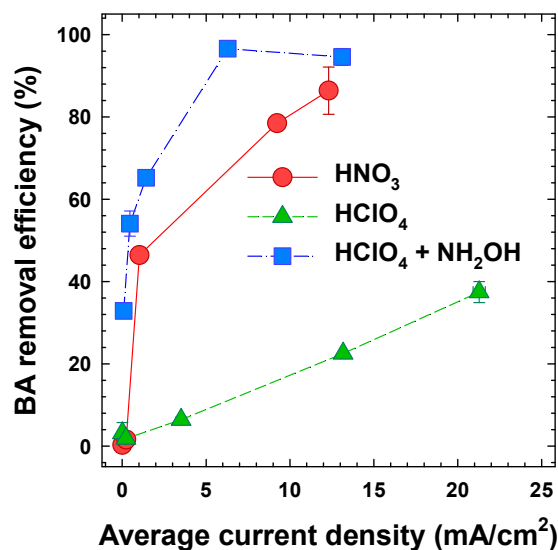
**Figure 14.** BA removal rate according to applied voltage with various electrolytes (Working electrode = platinum foil, counter electrode = titanium foil, reference electrode = saturated calomel electrode, effective electrode area = 10 cm<sup>2</sup>, pH<sub>i</sub> = 1.3, [Perchlorate]<sub>0</sub> = [Nitrate]<sub>0</sub> = 0.05 M, [Hydroxylamine]<sub>0</sub> = 5.0 mM, [Benzoic acid]<sub>0</sub> = 0.1 mM, reaction time = 2 hour, BA removal rate was calculated by initial phase of reaction).

Figure 14 shows the BA removal rate according to the applied voltage. In the case of the perchlorate electrolyte, the removal rate of BA increased depending on the applied voltage, albeit not significantly. However, in the case of the nitrate electrolyte condition, the removal rate of BA was greatly increased as the applied voltage increased. The perchlorate with HA electrolyte achieved the highest decomposition rate from 1.4 to 1.8 V vs. SCE, but the increase in rate within that voltage range was insignificant. However, after 1.8 V vs. SCE, the increase in BA removal rate was much larger and the trend in the change was similar to the nitrate electrolyte. This is related to the electrochemical behavior of the consumed HA, which is explained later on.



**Figure 15.** BA removal efficiency according to applied voltage with various electrolytes (Working electrode = platinum foil, counter electrode = titanium foil, reference electrode = saturated calomel electrode, effective electrode area = 10 cm<sup>2</sup>, pH<sub>i</sub> = 1.3, [Perchlorate]<sub>0</sub> = [Nitrate]<sub>0</sub> = 0.05 M, [Hydroxylamine]<sub>0</sub> = 5.0 mM, [Benzoic acid]<sub>0</sub> = 0.1 mM, reaction time = 2 hour, Coulombic efficiency of BA removal was calculated using final data point of each voltage condition.).

Figure 15 shows the coulombic efficiency of BA according to the applied voltage. Although the coulombic efficiency of BA was below 4.6% for all the electrolytes, it was confirmed that the level was always in the order of perchlorate with HA > nitrate > perchlorate regardless of voltage. This agrees with the results in Figure 14 in that HA had a positive effect on the electrochemical removal of BA.



**Figure 16.** BA removal efficiency according to average current density with various electrolytes (Working electrode = platinum foil, counter electrode = titanium foil, reference electrode = saturated calomel electrode, effective electrode area = 10 cm<sup>2</sup>, pH<sub>i</sub> = 1.3, [Perchlorate]<sub>0</sub> = [Nitrate]<sub>0</sub> = 0.05 M, [Hydroxylamine]<sub>0</sub> = 5.0 mM, [Benzoic acid]<sub>0</sub> = 0.1 mM, reaction time = 2 hour, BA removal efficiency was calculated using final data point of each voltage condition.).

Figure 16 shows the BA removal efficiency according to the average current density. When the same current was applied, the BA removal efficiency was in the electrolytic order of perchlorate with HA > nitrate > perchlorate. In addition, the extrapolated results (data not shown) suggest that the current density enabling 90% removal of 0.1 mM BA was estimated as 50 mA/cm<sup>2</sup> for perchlorate with HA, 15.7 mA/cm<sup>2</sup> for nitrate, and 5.25 mA/cm<sup>2</sup> for perchlorate during 2 hours of electrolysis. This indicates that HA reduced the energy consumption for the BA removal compared with perchlorate only.

### 3.2.3 Oxidation pathways

To compare the BA removal according to different electrolytes under constant voltage conditions and to understand the electrochemical behavior of HA, BA decomposition was depicted as electron consumption in coulombs.

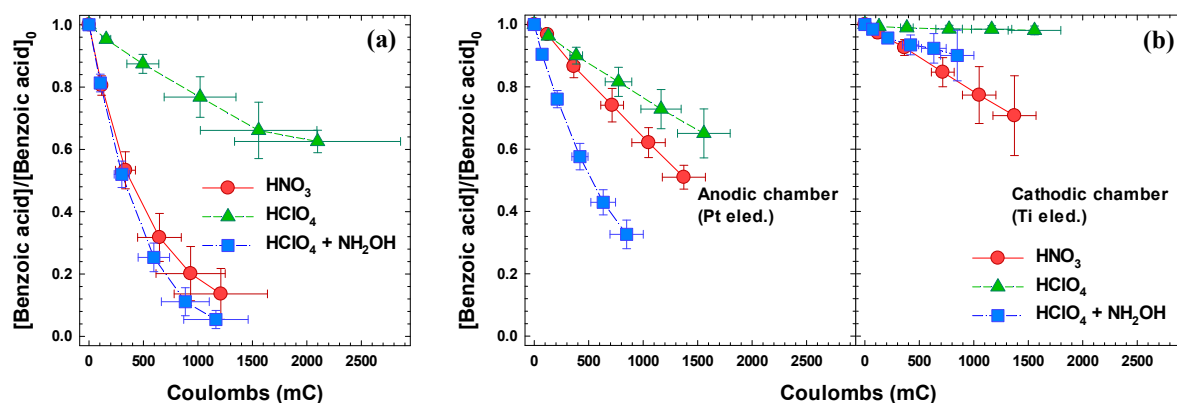


**Figure 17.** BA removal by electrolysis in two-chambered reactor (a) without PEM and (b) with PEM (Working electrode = platinum foil, counter electrode = titanium foil, reference electrode = saturated calomel electrode, effective electrode area = 10 cm<sup>2</sup>, applied potential = 2.2 V vs. SCE, pH<sub>i</sub> = 1.3, [Perchlorate]<sub>0</sub> = [Nitrate]<sub>0</sub> = 0.05 M, [Hydroxylamine]<sub>0</sub> = 5.0 mM, [Benzoic acid]<sub>0</sub> = 0.1 mM, reaction time = 2 hour).

In electrolysis experiments without a PEM (Figure 17(a)), the one with nitrate electrolyte achieved 86% BA removal during 1,210 mC of electron consumption, while the one with perchlorate consumed more electrons (2,098 mC) with less BA removal (37%). However, in the experiment with the perchlorate with HA electrolyte, the removal of BA increased to 94% and the consumption of electrons decreased to 1,165 mC, thereby showing a similar BA removal trend to the nitrate electrolyte. Thus, HA had a positive effect on BA removal and incurred a reduction in electron consumption during the electrolytic removal of BA.

To observe the electrochemical behavior of HA in detail, experiments were carried out with a PEM to separate the anodic and cathodic chambers (Figure 17(b)). PEM enabled individual observations of the oxidation and reduction reactions. In the case of the perchlorate electrolyte, the removal efficiency in the anodic chamber (35%) was similar to that of the two-chambered cell without a PEM (37%). In addition, the removal was observed in the anodic chamber only with negligible removal in the cathodic chamber (2%). Therefore, the BA decomposition in the perchlorate electrolyte was attributed to direct

oxidation by the anode since perchlorate is an electrochemically inert electrolyte under these conditions. In the case of perchlorate with HA, the BA removal was mostly observed in the anodic chamber (67%) with 10% in the cathodic chamber during 848 mC of electrons consumed. Compared with perchlorate only, it appears that there was around 32% and 8% improvement on BA removal in the anodic and cathodic chambers, respectively, which was believed to be due to the electrochemical activation of HA at the electrode.

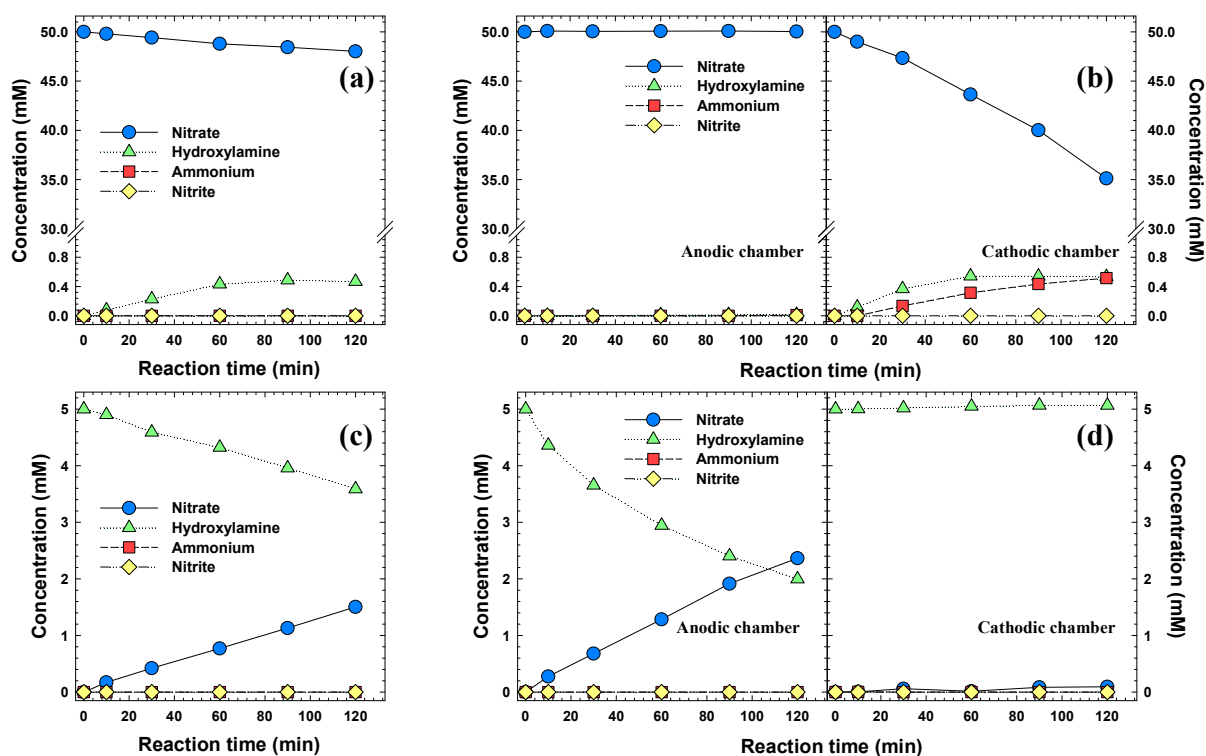
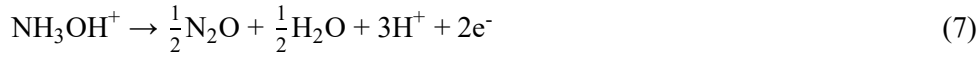


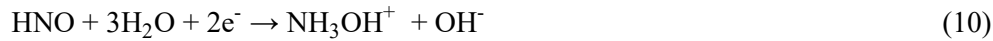
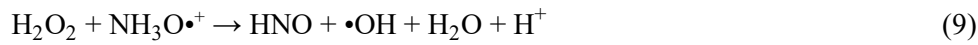
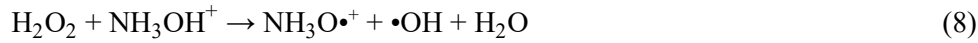
**Figure 18.** Concentration changes of N-species during hydroxylamine electrolysis in two-chambered reactor (Working electrode = platinum foil, counter electrode = titanium foil, reference electrode = saturated calomel electrode, effective electrode area = 10 cm<sup>2</sup>, applied potential = 2.2 V vs. SCE, pH<sub>i</sub> = 1.3, [Nitrate]<sub>0</sub> = [Perchlorate]<sub>0</sub> = 0.05 M, [Hydroxylamine]<sub>0</sub> = 5.0 mM, [Benzoic acid]<sub>0</sub> = 0.1 mM).

An increase in nitrate concentration was observed at the anodic chamber during the electrochemical activation of HA (Figure 18d) in agreement with Piela and Wrona<sup>16</sup> and it suggests the following reaction (6).



HA was oxidized at the anode to produce nitrate and hydroxyl radicals (the details are discussed later on). Some portion of the HA was oxidized and eliminated as the gaseous state since the total summation of nitrogen species decreased (the initial summation of nitrogen species (5 mM of HA) > the final summation of nitrogen species (4.4 mM (2.4mM of nitrate + 2.0 mM of HA))). The major gaseous nitrogen species in reaction (7) is dinitrogen oxide gas, as has been reported in previous research.<sup>23</sup>

10% of BA decomposition was confirmed at the reducing electrode, which is believed to be due to the following reactions:



Chen et al.<sup>30</sup> reported the reaction between  $\text{H}_2\text{O}_2$  and HA (reactions (8–10)). In their study, the kinetics of BA removal via reactions (8) and (9) was observed to be slow; the batch experiments in the present study attained similar results (Figure 19). However, in Figure 17(b), the kinetics are somewhat faster than Chen et al.'s results, which suggests that reactions (8) and (9) could be accelerated by electrode materials like Ti and Pt. However, additional experiments proved that there was no catalytic effect of the electrode material (Figure 20). Therefore, it is still possible that there was an electrocatalytic effect at the electrode surface that requires further investigation.



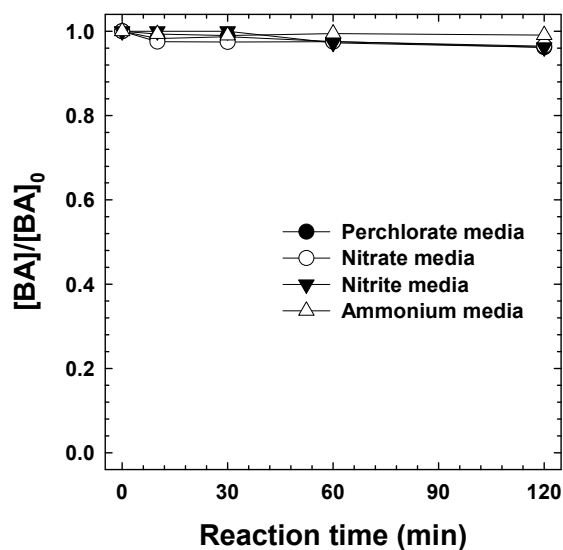


**Figure 19.** BA degradation by hydroxylamine/hydrogen peroxide upon various electrolytes ( $\text{pH}_i = 1.3$ ,  $[\text{Nitrate}]_0 = [\text{Nitrite}]_0 = [\text{Ammonium hydroxide}]_0 = 0.05 \text{ M}$ ,  $[\text{Benzoic acid}]_0 = 0.1 \text{ mM}$ ,  $[\text{Hydroxylamine}]_0 = 5.0 \text{ mM}$ ,  $[\text{Hydrogen peroxide}]_0 = 10.0 \text{ mM}$ ,  $\text{pH}_i$  was adjusted by perchloric acid except nitrate media condition)

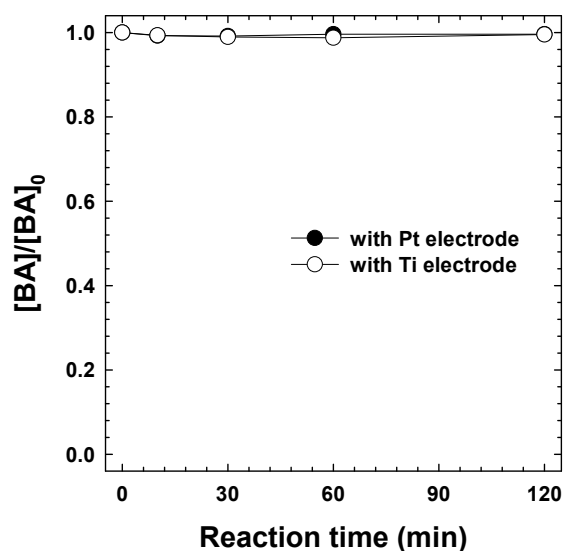
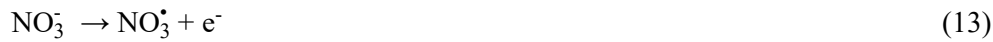


**Figure 20.** BA degradation by metal/hydroxylamine/hydrogen peroxide ( $\text{pH}_i = 1.3$ ,  $[\text{Nitrate}]_0 = 0.05 \text{ M}$ ,  $[\text{Benzoic acid}]_0 = 0.1 \text{ mM}$ ,  $[\text{Hydroxylamine}]_0 = 2.0 \text{ mM}$ ;  $[\text{Hydrogen peroxide}]_0 = 0.2 \text{ mM}$ )

Since ammonia was not observed, reaction (11)<sup>24</sup> appears to be negligible. Therefore, the major oxidant is thought to have been hydroxyl radicals produced via the electrocatalytic reaction between HA and H<sub>2</sub>O<sub>2</sub>. During reactions (8) and (9), the produced nitroxyl (HNO) could be reduced to HA, which could then participate in the oxidant generation reaction again.

In the two-compartment cell with a PEM and the nitrate electrolyte, there was 49% and 29% removal of BA at the anode and cathode, respectively, while for the perchlorate electrolyte, there was 35% BA removal at the anode. For the perchlorate electrolyte, the reaction of perchlorate ion is difficult since it is a fully oxidized form of chloride with oxygen, so direct oxidation and indirect oxidation-mediated hydroxyl radicals (reaction (12)) are the only possible pathways for BA removal. However, nitrate ions in the nitrate electrolyte can be further converted into nitrate radicals (reactions (13)<sup>40</sup> and (14)<sup>4</sup>), so there is an additional pathway for BA removal compared with perchlorate electrolyte in the anodic chamber:



On the other hand, the removal of BA in the cathodic chamber is achieved by the reaction between the reduction product of nitrate and oxygen. In the cathodic chamber with the perchlorate electrolyte, there was no direct reductive removal of BA by the cathode, thus the removal of BA could be attributed to a chemical reaction between the electrochemically generated molecules. First, in the cathodic chamber, the following possible reactions might have occurred:





These reactions are the electrochemical reduction reactions of the electrolyte components (reactions (15–18)) and the chemical reaction between the reduction products (reaction (19)) in the cathodic chamber. There are many other reactions including nitrogen gas, nitrous oxide, and nitric oxide, but they are not covered here to focus on the oxidant generation pathway during the electrochemical nitrate reduction process. Reactions (15–18) are well-known for nitrate and oxygen reduction, while reaction (19) is known as a Ti-catalyzed reaction.<sup>41,42</sup> The high HA production efficiency of the Ti electrode could be attributed to this chemical reaction catalyzed by the Ti electrode surface.

In the cathodic chamber, the nitrate electrolyte further removed around 27% of the BA compared to the perchlorate with HA electrolyte. Since HA was also formed in the cathodic chamber of the nitrate electrolyte condition, 10% of the total 29% removal rate appears to have been due to oxidant originating from HA and  $\text{H}_2\text{O}_2$  according to reactions (8) and (9). For the residual 19% of BA removal, the following equations are proposed:



ONOOH can be produced by the reaction of nitrite and  $\text{H}_2\text{O}_2$  (reaction (20)),<sup>36</sup> and can be reduced again at the cathode surface to produce nitrogen dioxide radical ( $\text{NO}_2^\bullet$ ) (reaction (21)),<sup>43</sup> or can be split into hydroxyl radicals and  $\text{NO}_2^\bullet$  (reaction (22))<sup>44</sup> in the bulk solution. Not only hydroxyl radicals, but also  $\text{NO}_2^\bullet$  can act as an oxidant. Additional experiments confirmed that ONOOH could have been involved in this system (Figure 21). Although nitrite (a precursor of ONOOH) was observed in the comparison of the cathode materials (Figure 7), nitrite was not observed in the BA removal experiment with a PEM (Figure 18 (b)). This could have been caused by the difference in the electrochemical

experimental conditions or the effect of BA. Therefore, it seems that ONOOH was not a major oxidant species in the cathodic compartment, which is also supported by the ESR results in Figure 24; no DMPO-X signal which is related to ONOOH were observed during the electrolysis.

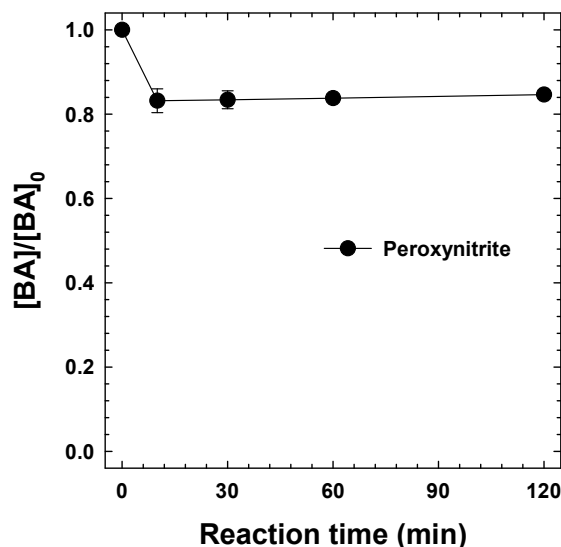


**Figure 21.** BA degradation by peroxynitrite (For peroxynitrite experiment:  $\text{pH}_i = 1.3$ ,  $[\text{Perchlorate}]_0 = 0.05 \text{ M}$ ,  $[\text{Peroxynitrite}]_0 = 10.0 \text{ mM}$ ,  $[\text{Benzoic acid}]_0 = 0.1 \text{ mM}$ )

The experimental results so far indicate that HA had a definite effect on electrolytic BA degradation and that the reaction occurred from HA's anodic oxidation. During the nitrate reduction process, the BA removal pathway could be categorized into major three groups: (1) by the anode and the anodic product, (2) by the anode and the cathodic product HA, and (3) by the cathode and the cathodic product. Each group includes the respective following specific reactions mentioned previously: group (1), direct oxidation and nitrate radicals; group (2), anodic activation of HA; and group (3) between the reduction products (nitrite,  $\text{H}_2\text{O}_2$ , and HA). Each group could be estimated from the experimental results of the separated electrochemical cell with and without a PEM since the electrochemical reaction proceeded as measured by the coulombic value. Thus, the comparison of BA removal at the same coulombic value made it possible to determine the percentage responsibility of each group for each electrolyte.

For the nitrate electrolyte, BA removal was 87% at 1,220 C without a PEM and 43% and 26% in the anodic and cathodic chambers for the same coulombic value with a PEM, respectively. From a comparison of the BA removal results, the percentage responsibility of each group was calculated using the following process. In the anodic chamber, group (1) was responsible for BA removal at 49.4% (43/87). In the cathodic chamber, group (3) was responsible for BA removal at 29.9% (26/87). Thus, the percentage responsibility of group (2) comprises the remainder: total responsibility (100%) – (responsibility of group (1) (49.4) - responsibility of group (3) (29.9%)) = 20.7%.

### III. Identification of the oxidant species

Although BA is known as a probe compound for hydroxyl radicals since it is difficult to decompose it effectively via other oxidants, a scavenger test and ESR measurements were performed to identify the oxidant species produced in each electrolyte (Figures 22–30).

#### 3.3.1 Scavenger test

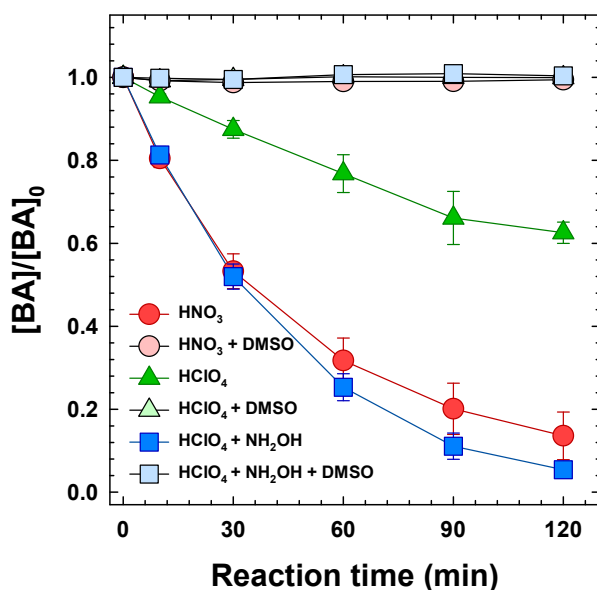


**Figure 22.** Effect of DMSO on various electrolytes during electrolysis (Working electrode = platinum foil, counter electrode = titanium foil, reference electrode = saturated calomel electrode, effective electrode area = 10 cm<sup>2</sup>, applied potential = 2.2 V vs. SCE, pH<sub>i</sub> = 1.3, [Perchlorate]<sub>0</sub> = [Nitrate]<sub>0</sub> = 0.05 M, [Hydroxylamine]<sub>0</sub> = 5.0 mM, [Benzoic acid]<sub>0</sub> = 0.1 mM, [DMSO]<sub>0</sub> = 200 mM).

Figure 22 shows the effect of the scavenger, DMSO, during the BA electrolysis in the three electrolytes. DMSO is a well-known hydroxyl radical scavenger and was adopted to identify whether the hydroxyl radical was the main oxidant or not. As expected, BA removal was completely scavenged by DMSO in all three electrolytes, thus the oxidizing agent generated in each electrochemical system is assumed to have comprised hydroxyl radicals. To collect more solid evidence, ESR experiments were conducted additionally.

### 3.3.2 ESR spectroscopy

ESR spectroscopy is one of the qualitative analyses for identifying radical species with a very short lifetime, which makes it difficult to detect them via a conventional analysis. Radical species react with a spin-trap agent to form a spin-adduct with a relatively longer lifetime, which makes it possible to qualitatively analyze them. In the case of hydroxyl radicals, DMPO is known to form a relatively stable spin-adduct, DMPO-OH. In this study, DMPO was used to identify the oxidant in the system. In addition, a quantitative comparison of oxidant generation was performed through a comparison of signal intensity.

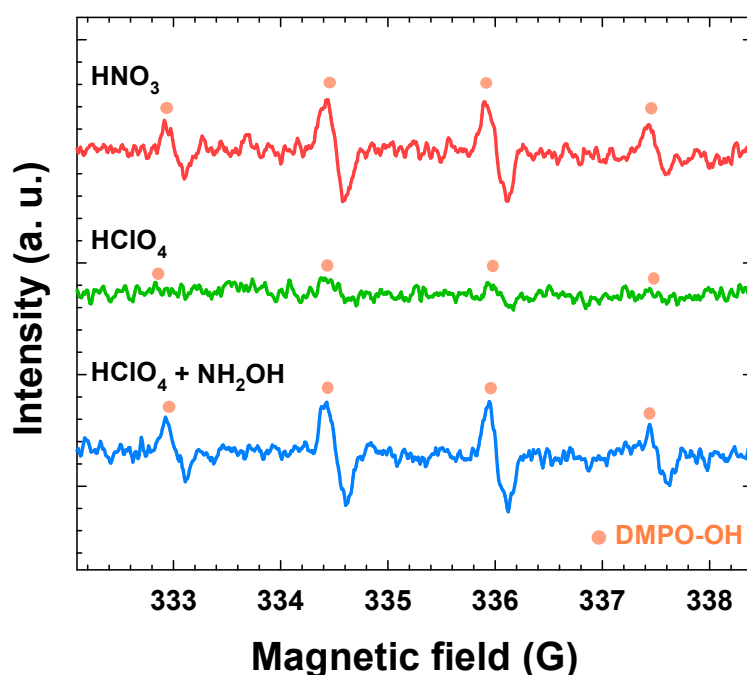


**Figure 23.** ESR spectra obtained by spin trapping with DMPO during electrolysis (Working electrode = platinum foil, counter electrode = titanium foil, reference electrode = saturated calomel electrode, effective electrode area = 10 cm<sup>2</sup>, applied potential = 2.2 V vs. SCE, pH<sub>i</sub> = 1.3, [Perchlorate]<sub>0</sub> = [Nitrate]<sub>0</sub> = 0.05 M, [Hydroxylamine]<sub>0</sub> = 5.0 mM, [Benzoic acid]<sub>0</sub> = 0.1 mM, [DMPO]<sub>0</sub> = 5.0 mM, ESR signal was obtained after 5 seconds).

Figure 23 shows the clear DMPO-OH ESR signal obtained for each electrolyte; any other signals for species like DMPO-O<sub>2</sub><sup>•</sup> and DMPO-X were not observed during the 2 hours of electrolysis. It is known that DMPO-O<sub>2</sub><sup>•</sup> can be generated from the superoxide radical and DMPO-X can come about under strong oxidative conditions or an electron transfer reaction with DMPO. In this study, the DMPO-X signal was only obtained from the ONOOH experiment (Figure 24), which supports that ONOOH is not a major oxidant species during the electrolysis of HA with the perchlorate or nitrate electrolytes.

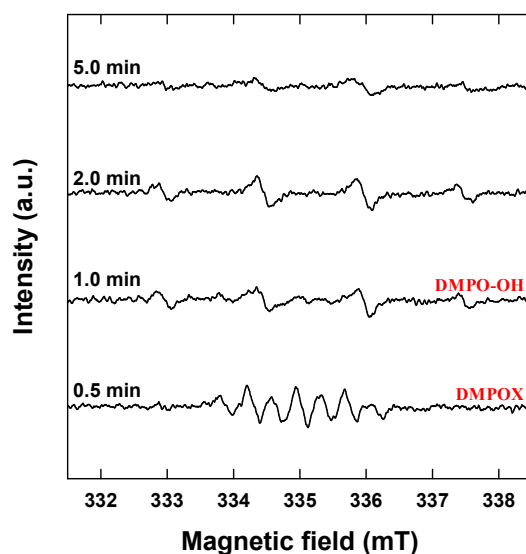


**Figure 24.** ESR signals of DMPO spin trapping adducts produced by peroxynitrite ( $\text{pH}_i = 1.5$ ,  $[\text{peroxynitrite}]_0 = 10.0 \text{ mM}$ ,  $[\text{DMPO}]_0 = 10.0 \text{ mM}$ )

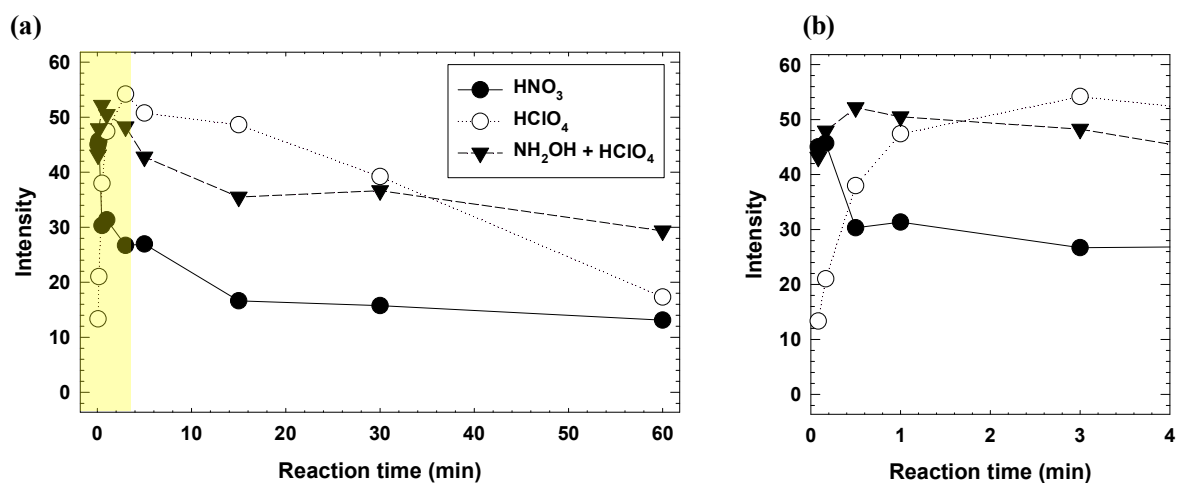


**Figure 25.** (a) ESR intensity obtained by spin trapping with DMPO during electrolysis and (b) initial part of result (Working electrode = platinum foil, counter electrode = titanium foil, reference electrode = saturated calomel electrode, effective electrode area =  $10 \text{ cm}^2$ , applied potential =  $2.2 \text{ V}$  vs. SCE,  $\text{pH}_i = 1.3$ ,  $[\text{Perchlorate}]_0 = [\text{Nitrate}]_0 = 0.05 \text{ M}$ ,  $[\text{Hydroxylamine}]_0 = 5.0 \text{ mM}$ ,  $[\text{Benzoic acid}]_0 = 0.1 \text{ mM}$ ,  $[\text{DMPO}]_0 = 5.0 \text{ mM}$ ).

These results strongly support the generation of hydroxyl radicals from the electrochemical oxidation of HA and during the electrochemical nitrate reduction process. At the initial of electrolysis, the order of intensity for each electrolyte was perchlorate with HA > nitrate > perchlorate. However, the intensity of the ESR signals increased at the very beginning of the electrolysis and decreased over time. To clarify this tendency, the intensity change over time is shown in Figure 25.

The nitrate electrolyte had a tendency to decrease continuously over time, while the perchlorate electrolyte signal increased up to 3 minutes and then decreased drastically. The HA added perchlorate electrolyte condition was similar to the nitrate electrolyte, but its overall intensities were higher. The reason for the increased signal intensity is believed to be due to the generated DMPO-OH spin-adduct from the reaction of DMPO and the hydroxyl radicals. Moreover, the reason for the decrease after the increase is believed to be due to the natural electrochemical decaying of DMPO-OH.

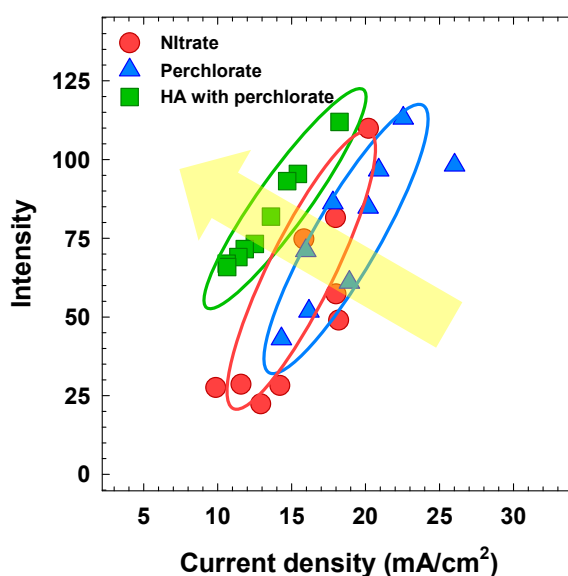


**Figure 26.** ESR intensity according to current density (Working electrode = platinum foil, counter electrode = titanium foil, reference electrode = saturated calomel electrode, effective electrode area = 10 cm<sup>2</sup>, applied potential = 2.2 V vs. SCE, pH<sub>i</sub> = 1.3, [Perchlorate]<sub>0</sub> = [Nitrate]<sub>0</sub> = 0.05 M, [Hydroxylamine]<sub>0</sub> = 5.0 mM, [Benzoic acid]<sub>0</sub> = 0.1 mM, [DMPO]<sub>0</sub> = 5.0 mM).

Since the results described previously were obtained under a constant voltage, the current was different depending on the electrolyte condition and also changed as the electrolysis progressed. Therefore, the interpretation of ESR signal intensity over time cannot be used to quantitatively measure hydroxyl radical generation properly. To compare the amount of hydroxyl radical generation according to the electrolyte, Figure 25 was converted to current density vs. intensity of DMPO-OH, the results for



which are presented in Figure 26; the HA added perchlorate electrolyte attained a higher DMPO-OH signal intensity with a lower current density and nitrate concentration. This result implies that HA produced more hydroxyl radicals with a smaller applied current (in other words, the order of current efficiency of hydroxyl radical generation was perchlorate with HA > nitrate > perchlorate). This supports the results in Figure 16.

#### IV. Applicability of this study to wastewater treatment

Electrochemical HA production is one of the significant parts of this study. Based on this, it is possible to combine it with any system which requires the external injection of HA, such as the Cu/H<sub>2</sub>O<sub>2</sub>/HA<sup>23</sup> PMS/HA<sup>32</sup> systems. The following experiments were conducted to evaluate its applicability further.

##### 3.4.1 Application in various pH regions

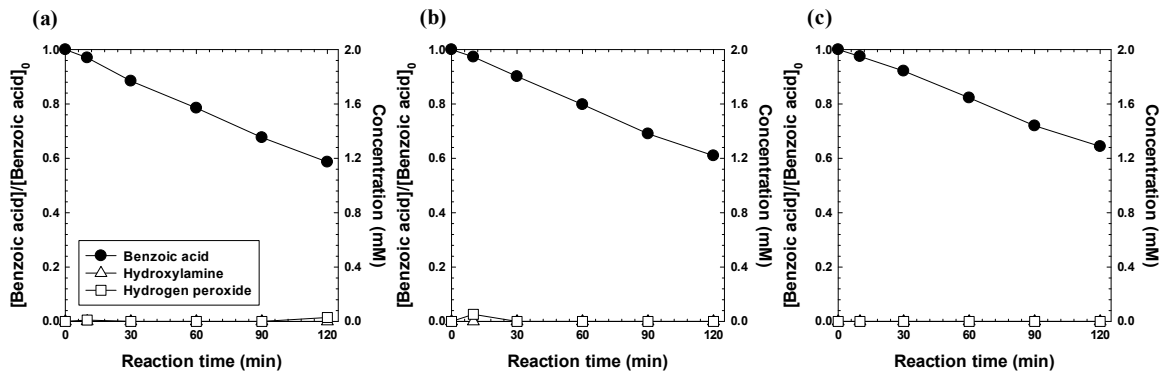


**Figure 27.** BA degradation by electrolysis of perchlorate electrolyte at (a) pH 1.5, (b) 7.0, and (c) 12.5 (Cathode = Titanium foil, Anode = Platinum foil,  $\text{pH}_i = 1.5, 7.0$  and  $12.5$ , Effective electrode area =  $10 \text{ cm}^2$ ,  $[\text{Perchlorate}]_0 = 0.05 \text{ M}$ ,  $[\text{Benzoic acid}]_0 = 0.1 \text{ mM}$ , Applied current density =  $30 \text{ mA/cm}^2$ )

Basically, the perchlorate electrolyte is electrochemically inert, so other oxidant generation pathways except for water electrolysis producing hydroxyl radicals are not expected, making it more difficult to decompose BA compared with the other electrolytes in this study. This was also the case in other pH regions (neutral and basic) (Figure 27).

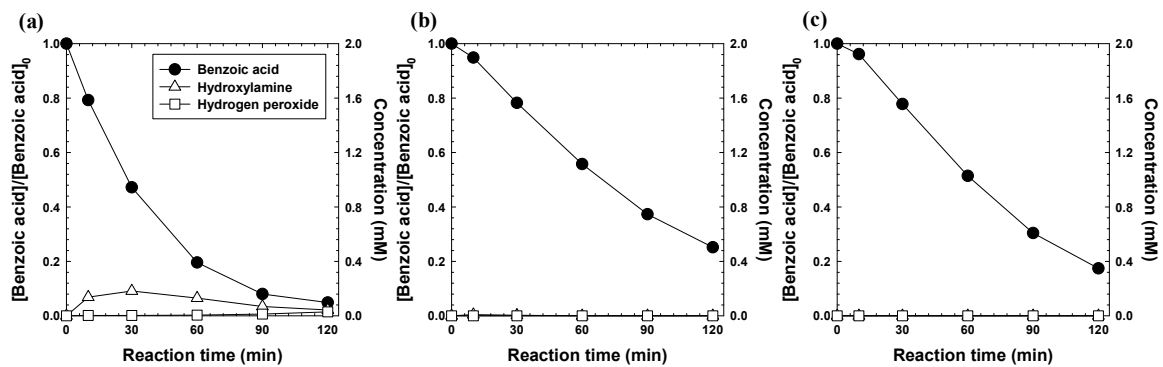


**Figure 28.** BA degradation by electrolysis of nitrate electrolyte at (a) pH 1.5, (b) 7.0, and (c) 12.5 (Cathode = Titanium foil, Anode = Platinum foil,  $\text{pH}_i = 1.5, 7.0$  and  $12.5$ , Effective electrode area =  $10 \text{ cm}^2$ ,  $[\text{Nitrate}]_0 = 0.05 \text{ M}$ ,  $[\text{Benzoic acid}]_0 = 0.1 \text{ mM}$ , Applied current density =  $30 \text{ mA/cm}^2$ )

The nitrate electrolyte attained a better decomposition rate than the perchlorate electrolyte in the neutral and basic pH regions (Figure 28), but this was lower than in the acidic pH region. It is considered that HA is not produced at a pH of over 2.0, and the hydroxyl radical generation pathway from the electrochemical oxidation of HA had disappeared, leading to a lower removal rate and efficiency. Nonetheless, the BA removal efficiency and rate were higher than for the perchlorate electrolyte, which is attributed to the nature of the electrolyte oxidant generation pathway mentioned in Section 3.2.3.

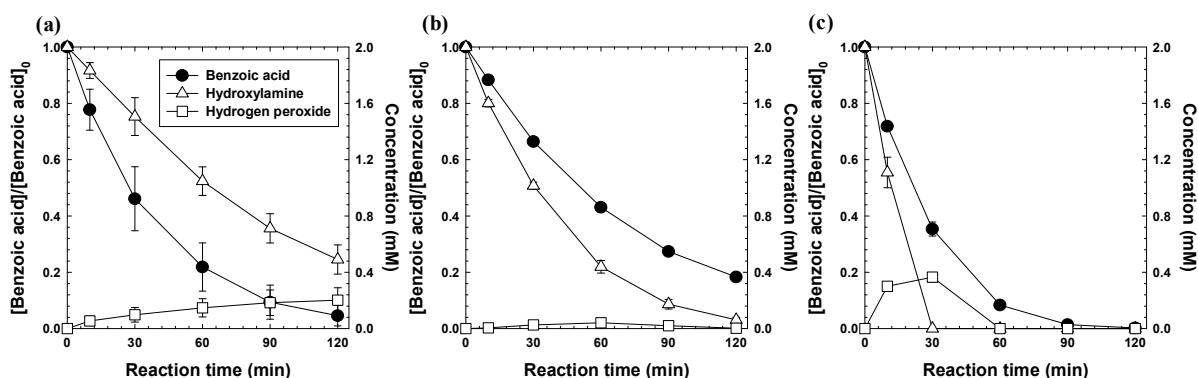


**Figure 29.** BA degradation by electrolysis of HA added electrolyte at (a) pH 1.5, (b) 7.0, and (c) 12.5 (Cathode = Titanium foil, Anode = Platinum foil,  $pH_i = 1.5, 7.0$  and  $12.5$ , Effective electrode area =  $10\text{ cm}^2$ ,  $[Perchlorate]_0 = 0.05\text{ M}$ ,  $[Hydroxylamine]_0 = 2.0\text{ mM}$ ,  $[Benzoic\ acid]_0 = 0.1\text{ mM}$ , Applied current density =  $30\text{ mA/cm}^2$ )

For the perchlorate with HA electrolyte, the BA removal rate slowed down in the neutral pH region, albeit still faster than the others, and accelerated again in the basic pH region; the increase in BA removal rate and efficiency was noticeable. In addition, a rapid decrease in HA was observed in the basic pH region, probably from a reaction between a base and HA. From the experimental results, it was confirmed that BA degradation by HA was improved irrespective of the pH region (Figure 29).

### 3.4.2 Simultaneous removal of nitrate and organic pollutants

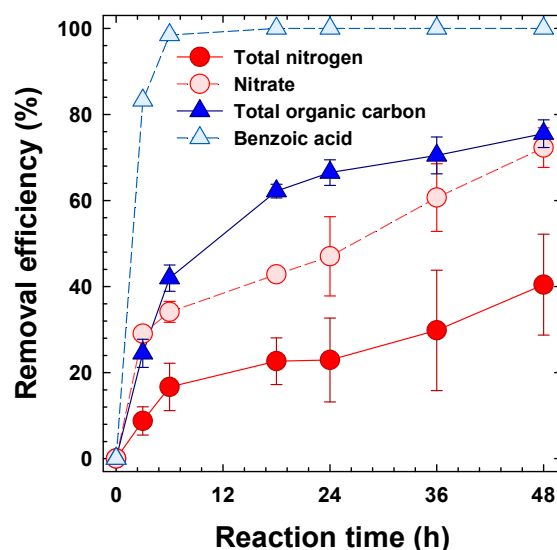


**Figure 30.** Simultaneous removal of nitrate and organic pollutants during nitrate reduction process (Anode = platinum foil, cathode = titanium foil, effective electrode area = 10 cm<sup>2</sup>, current density = 30 mA/cm<sup>2</sup>, pH<sub>i</sub> = 2.0, [Nitrate]<sub>0</sub> = 800 ppm, [Benzoic acid]<sub>0</sub> = 100 ppm ([Nitrate]<sub>0</sub> = 12.9 mM, [Benzoic acid]<sub>0</sub> = 0.82 mM)).

Generally, nitrates are removed by reduction and organic pollutants by oxidation; electrochemical processes can comprise reduction and oxidation reactions, and so are promising for simultaneous nitrate and organic pollutant removal. Despite the feasibility of electrochemical nitrate reduction for simultaneous control of nitrate and organic pollutants, only a little amount of research has been conducted on this, most of which has been to use biological/bioelectrochemical (like anaerobic processes and microbial fuel cells)<sup>45-54</sup> and membrane (like ultrafiltration and reverse osmosis)<sup>55,56</sup> technology.

The results of this study suggest an innovative electrochemical process for the simultaneous removal of nitrate and organic pollutants. Nitrates could be reductively removed at the cathode and organic pollutants could be oxidatively removed at the anode. During the suggested process, an intermediate (in this study, HA) generated from the electrochemical nitrate reduction could enhance BA removal while alleviating the nitrate concentration.

In a laboratory-scale demonstration of the process, the simultaneous removal of nitrate and organic pollutants along with TOC and TN was observed (Figure 30). The BA molecules were completely degraded within 6 hours, and the degradation products were mineralized into carbon dioxide, reducing TOC by 76% within 48 hours. The removal of nitrate decreased rapidly until 3 hours, then decreased

relatively constantly; finally, 72% was removed. TN was the most difficult to remove; it decreased rapidly until 6 hours, then slowly decreased; finally, 40% was removed. However, for the optimization of this system, it would be necessary for more studies involving electrochemical configurations (electrode area / reactor volume ratio, anion effect in the electrolyte, and ETCs) and composite electrode materials (anodes with higher oxidant conversion of HA, cathodes with higher selectivity of HA, and gaseous nitrogen species).

## Chapter 4. Conclusions

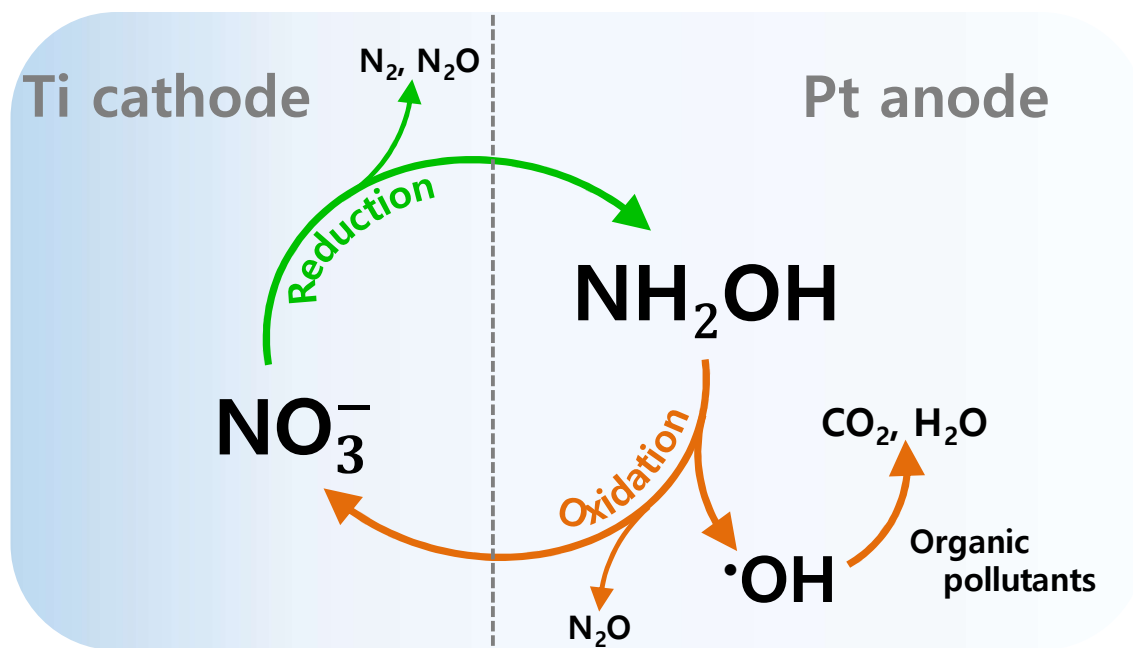


**Figure 31.** Scheme of electrochemical removal of nitrate and organic pollutant

In this study, a process capable of degrading refractory organic pollutants using nitrate ions was developed. HA was introduced as the main intermediate produced from the electrochemical reduction of nitrate and it was electrochemically utilized to degrade BA. During the process, HA was electrochemically activated, producing hydroxyl radicals as the main oxidant (Figure 31).

The electrochemical generation of HA was investigated in the first part of the study. HA is a reactive chemical with considerable potential for producing reactive oxidant species with proper activation. To electrochemically produce HA from nitrate ions, various electrochemical conditions and cathode materials were tested. From the experimental results, it was found that the electrochemical production of HA requires proper current density and an acidic pH. Moreover, it was confirmed that the Ti cathode could electrochemically generate HA efficiently and the Sn cathode could predominantly generate HA while producing fewer ions like nitrite and ammonium. As a result, Ti was chosen as the optimal cathode material for the developed process.

Second, the performance of the process was evaluated via BA degradation in three electrolytes: nitrate, perchlorate, and perchlorate with HA. BA removal drastically higher for the nitrate electrolyte compared with the perchlorate electrolyte, which was similar to the comparison between the latter and the perchlorate with HA electrolyte. The electrochemical reduction of nitrate enhanced BA removal and HA accounted for 20% of the BA removal.

Third, the electrochemical behavior of HA was investigated. The electrochemical activation of HA was observed at the anode and the final product after activation of HA was identified as nitrates. Through a scavenger test and ESR spectroscopy, the generated oxidant species from the electrochemical activation of HA was confirmed as hydroxyl radicals. The proposed scheme is described in Figure 31.

Finally, the applicability of the process was examined. Various pH conditions were tested and BA removal efficiencies were investigated. Compared with the perchlorate electrolyte, the nitrate and HA with perchlorate electrolytes attained enhanced BA removal efficiency. In addition, the potential for simultaneous removal of nitrate and organic pollutants was assessed, and although the rate of removal was not high, the simultaneous removal of nitrate and organic pollutants was accomplished.

## References

1. Anglada, A.; Urtiaga, A.; Ortiz, I., Contributions of electrochemical oxidation to waste-water treatment: fundamentals and review of applications. *J. Chem. Technol. Biotechnol.* **2009**, 84 (12), 1747-1755.
2. Radjenovic, J.; Sedlak, D. L., Challenges and Opportunities for Electrochemical Processes as Next-Generation Technologies for the Treatment of Contaminated Water. *Environ. Sci. Technol.* **2015**, 49 (19), 11292-302.
3. Sharma, V. K.; Oxidation of inorganic contaminants by ferrates (VI, V, and IV)-kinetics and mechanisms: A review. *J. Environ. Management* **2011**, 92(4), 1051-1073.
4. Neta, P.; Huie, R. E.; Ross, A. B.; Rate constants for reactions of inorganic radicals in aqueous solution. *J. Phys. Chem. Ref. Data.* **1988**, 17(3), 1027-1284.
5. Lide, D. R. Eds. *CRC Handbook of Chemistry and Physics, Internet Version*; CRC press: Florida, U.S., 1993.
6. Spiro, M.; The standard potential of the peroxosulphate/sulphate couple. *Electrochim. Acta*, **1979**, 24(3), 313-314.
7. Zayed, G.; Winter, J., Removal of organic pollutants and of nitrate from wastewater from the dairy industry by denitrification. *Appl. Microbiol. Biotechnol.* **1998**, 49, 469-474.
8. Shen, C.-w.; Tran, P.; Minh Ly, P., Chemical Waste Management in the U.S. Semiconductor Industry. *Sustainability* **2018**, 10 (5), 1545-1558.
9. Gowardhan, A. S.; Deshpande, S. D.; Chakrabarti, T., Biological degradation of high nitrate wastewater under anoxic conditions. *Int. J. Environ. Stud.* **1995**, 47 (2), 119-132.
10. Hussain, J.; Hussain, I.; Arif, M., Characterization of textile wastewater. *J. Ind. Pollut. Contr.* **2004**, 20 (1), 137-144.
11. Katsounaros, I.; Kyriacou, G., Influence of nitrate concentration on its electrochemical reduction on tin cathode: Identification of reaction intermediates. *Electrochim. Acta* **2008**, 53 (17), 5477-5484.



12. Katsounaros, I.; Dortsiou, M.; Polatides, C.; Preston, S.; Kypraios, T.; Kyriacou, G., Reaction pathways in the electrochemical reduction of nitrate on tin. *Electrochim. Acta* **2012**, 71, 270-276.
13. Davis, P.; Evans, M. G.; Higginson, W. C. E., Some oxidation–reduction reactions of hydroxylamine. *J. Chem. Soc.* **1951**, 2563-2567.
14. Carter, M. K.; Small, R. J., Radical Formation in Hydroxylamine-Copper Chemical Mechanical Planarization Processes. *J. Electrochem. Soc.* **2003**, 150 (2), G107-G111.
15. Ebadi, M., Electrocatalytic oxidation of hydroxylamine by (RuPc)<sub>2</sub> graphite modified electrode. *Electrochim. Acta* **2003**, 48 (28), 4233-4238.
16. Piela, B.; Wrona, P. K., Oxidation of Hydroxylamine on the Rotating Solid Electrodes. *J. Electrochem. Soc.* **2004**, 151 (2), E69-E79.
17. Rosca, V.; Beltramo, G. L.; Koper, M. T. M., Hydroxylamine Electrochemistry at Low-Index Single-Crystal Platinum Electrodes in Acidic Media. *J. Phys. Chem. B* **2004**, 108 (24), 8294-8304.
18. Godoi, D. R.; Chen, Y.; Zhu, H.; Scherson, D., Electrochemical oxidation of hydroxylamine on gold in aqueous acidic electrolytes: an in situ SERS investigation. *Langmuir* **2010**, 26 (20), 15711-15713.
19. Jebaraj, A. J. J.; de Godoi, D. R. M.; Scherson, D., The oxidation of hydroxylamine on Pt-, and Pd-modified Au electrodes in aqueous electrolytes: Electrochemical and in situ spectroscopic studies. *Catal. Today* **2013**, 202, 44-49.
20. Mazloumardkani, M.; Karami, P. E.; Naeimi, H.; Mirjalili, B., Electrocatalytic Oxidation of Hydroxylamine at a Quinizarine Modified Glassy Carbon Electrode: Application to Differential Pulse Voltammetry Detection of Hydroxylamine. *Turk. J. Chem.* **2008**, 32, 571-584.
21. Duca, M.; Koper, M. T. M., Powering denitrification: the perspectives of electrocatalytic nitrate reduction. *Energy Environ. Sci.* **2012**, 5 (12), 9726-9742.
22. Lee, H. J.; Kim, H. E.; Lee, C., Combination of cupric ion with hydroxylamine and hydrogen peroxide for the control of bacterial biofilms on RO membranes. *Water Res.* **2017**, 110, 83-90.

23. Lee, H.; Lee, H. J.; Seo, J.; Kim, H. E.; Shin, Y. K.; Kim, J. H.; Lee, C., Activation of Oxygen and Hydrogen Peroxide by Copper(II) Coupled with Hydroxylamine for Oxidation of Organic Contaminants. *Environ. Sci. Technol.* **2016**, 50 (15), 8231-8238.
24. Kim, H. E.; Nguyen, T. T.; Lee, H.; Lee, C., Enhanced Inactivation of *Escherichia coli* and MS2 Coliphage by Cupric Ion in the Presence of Hydroxylamine: Dual Microbicidal Effects. *Environ. Sci. Technol.* **2015**, 49 (24), 14416-14423.
25. Zou, J.; Ma, J.; Chen, L.; Li, X.; Guan, Y.; Xie, P.; Pan, C., Rapid acceleration of ferrous iron/peroxymonosulfate oxidation of organic pollutants by promoting Fe(III)/Fe(II) cycle with hydroxylamine. *Environ. Sci. Technol.* **2013**, 47 (20), 11685-11691.
26. Zhang, J.; Chen, M.; Zhu, L., Activation of peroxymonosulfate by iron-based catalysts for orange G degradation: role of hydroxylamine. *RSC Adv.* **2016**, 6 (53), 47562-47569.
27. Zhou, P.; Zhang, J.; Liang, J.; Zhang, Y.; Liu, Y.; Liu, B., Activation of persulfate/copper by hydroxylamine via accelerating the cupric/cuprous redox couple. *Water Sci Technol.* **2016**, 73 (3), 493-500.
28. Wu, X.; Gu, X.; Lu, S.; Qiu, Z.; Sui, Q.; Zang, X.; Miao, Z.; Xu, M.; Danish, M., Accelerated degradation of tetrachloroethylene by Fe(II) activated persulfate process with hydroxylamine for enhancing Fe(II) regeneration. *J. Chem. Technol. Biotechnol.* **2015**, 91 (5), 1280-1289.
29. Chen, L.; Ma, J.; Li, X.; Zhang, J.; Fang, J.; Guan, Y.; Xie, P., Strong enhancement on fenton oxidation by addition of hydroxylamine to accelerate the ferric and ferrous iron cycles. *Environ. Sci. Technol.* **2011**, 45 (9), 3925-3930.
30. Chen, L.; Li, X.; Zhang, J.; Fang, J.; Huang, Y.; Wang, P.; Ma, J., Production of Hydroxyl Radical via the Activation of Hydrogen Peroxide by Hydroxylamine. *Environ. Sci. Technol.* **2015**, 49 (17), 10373-10379.
31. Zhang, J.; Zhang, Y.-L.; Shi, Y.-N.; Lin, J.; Zhou, P.; Zhang, W.-Q.; Xu, J.-W., Acceleration of Ozone Decomposition and  $\cdot\text{OH}$  Generation by Hydroxylamine. *Ozone Sci Eng* **2016**, 38 (2), 150-155.
32. Feng, Y.; Wu, D.; Zhou, Y.; Shih, K., A metal-free method of generating sulfate radicals through direct interaction of hydroxylamine and peroxymonosulfate: Mechanisms, kinetics, and implications. *Chem. Eng. J.* **2017**, 330, 906-913.

33. Kono, Y., Generation of SUPeroxide Radical during Autoxidation of Hydroxylamine and an Assay for Superoxide Dismutase. *Arch. Biochem. Biophys.* **1978**, 186 (1), 189-195.
34. Neta, P.; Maruthamuthu, P.; Carton, P. M.; Fessenden, R. W., Formation and Reactivity of the Amino Radical. *J. Phys. Chem.* **1978**, 82 (17), 1875-1878.
35. Yagil, G.; Anbar, M., The Formation of Peroxynitrite by Oxidation of Chloramine, Hydroxylamine and Nitrohydroxamate. *J. Inorg. Nucl. Chem.* **1964**, 26, 453-460.
36. Robinson, K. M.; Beckman, J. S., Synthesis of Peroxynitrite from Nitrite and Hydrogen Peroxide. *Methods Enzymol.* **2005**, 396, 207-214.
37. Frear, D. S.; Burrell, R. C., Spectrophotometric Method for Determining Hydroxylamine Reductase Activity in Higher Plants. *Anal. Chem.* **1955**, 27 (10), 1664-1665.
38. Dortsiou, M.; Katsounaros, I.; Polatides, C.; Kyriacou, G., Influence of the electrode and the pH on the rate and the product distribution of the electrochemical removal of nitrate. *Environ. Technol.* **2013**, 34 (3), 373-381.
39. Montilla, F.; Michaud, P. A.; Morallón, E.; Vázquez, J. L.; Comninellis, C., Electrochemical oxidation of benzoic acid at boron-doped diamond electrodes. *Electrochim. Acta* **2002**, 47 (21), 3509-3513.
40. Tomat, R.; Rigo, A., Electrochemical oxidation of aliphatic hydrocarbons promoted by inorganic radicles. II. NO<sub>3</sub> radicles. *J. Appl. Electrochem.* **1986**, 16, 8-14.
41. Mantegazza, M. A.; Leofanti, G.; Petrini, G.; Padovan, M.; Zecchina, A.; Bordiga, S., Selective Oxidation of Ammonia to Hydroxylamine with Hydrogen Peroxide on Titanium Based Catalysts. *Studies in Surface Science and Catalysis* **1994**, 82, 541-550.
42. Sirijaraensre, J.; Limtrakul, J., Mechanisms of the ammonia oxidation by hydrogen peroxide over the perfect and defective Ti species of TS-1 zeolite. *Phys. Chem. Chem. Phys.* **2013**, 15 (41), 18093-18100.
43. Merenyi, G.; Lind, J., Free radical formation in the peroxynitrous acid (ONOOH)/peroxynitrite (ONOO<sup>-</sup>) system. *Chem. Res. Toxicol.* **1998**, 11 (4), 243-246.
44. Lobachev, V. L.; Rudakov, E. S., The chemistry of peroxynitrite. Reaction mechanisms and kinetics. *Russ. Chem. Rev.* **2006**, 75 (5), 375-396.

45. Saeedi, R.; Naddafi, K.; Nabizadeh, R.; Mesdaghinia, A.; Nasser, S.; Alimohammadi, M.; Nazmara, S., Simultaneous Removal of Nitrate and Natural Organic Matter from Drinking Water Using a Hybrid Heterotrophic/Autotrophic/Biological Activated Carbon Bioreactor. *Environ. Eng. Sci.* **2012**, 29 (2), 93-100.
46. Dhamole, P. B.; Nair, R. R.; D'Souza, S. F.; Lele, S. S., Simultaneous removal of carbon and nitrate in an airlift bioreactor. *Bioresour. Technol.* **2009**, 100 (3), 1082-1086.
47. Herzberg, M.; Dosoretz, C. G.; Tarre, S.; Michael, B.; Dror, M.; Green, M., Simultaneous removal of atrazine and nitrate using a biological granulated activated carbon (BGAC) reactor. *J. Chem. Technol. Biotechnol.* **2004**, 79 (6), 626-631.
48. Katz, I.; Dosoretz, C.; Ruskol, Y.; Green, M., Simultaneous removal of nitrate and atrazine from groundwater. *Water Sci. Technol.* **2000**, 41 (4-5), 49-56.
49. de Kreuk, M. K.; Heijnen, J. J.; van Loosdrecht, M. C., Simultaneous COD, nitrogen, and phosphate removal by aerobic granular sludge. *Biotechnol. Bioeng.* **2005**, 90 (6), 761-769.
50. Wang, X. M.; Qiu, T. L.; Gao, M.; Han, M. L.; Gao, J. L., Simultaneous Removal of Nitrate and Pentachlorophenol from Drinking Water Using Wheat Straw as Carbon Source. *Appl. Mech. Mater.* **2014**, 522, 596-599.
51. Yang, S.; Yao, G., Simultaneous removal of concentrated organics, nitrogen and phosphorus nutrients by an oxygen-limited membrane bioreactor. *PLoS One* **2018**, 13 (8), e0202179.
52. Zhu, J.-H.; Lin, J.-P.; Zhang, B.; Yan, X.-L.; Peng, Z.-G., Simultaneous Removal of Phenol and Nitrate in an Anaerobic Bioreactor. *J. Environ. Eng.* **2006**, 132 (9), 1073-1077.
53. Zhou, M.; Wang, W.; Chi, M., Enhancement on the simultaneous removal of nitrate and organic pollutants from groundwater by a three-dimensional bio-electrochemical reactor. *Bioresour. Technol.* **2009**, 100 (20), 4662-4668.
54. Viridis, B.; Rabaey, K.; Yuan, Z.; Keller, J., Microbial fuel cells for simultaneous carbon and nitrogen removal. *Water Res.* **2008**, 42 (12), 3013-3024.
55. Baek, K.; Yang, J. W., Simultaneous removal of chlorinated aromatic hydrocarbons, nitrate, and chromate using micellar-enhanced ultrafiltration. *Chemosphere* **2004**, 57 (9), 1091-1097.

56. Tepus, B.; Simonic, M.; Petrinic, I., Comparison between nitrate and pesticide removal from ground water using adsorbents and NF and RO membranes. *J. Hazard. Mater.* **2009**, 170 (2-3), 1210-1217.